Novel Benzofuran and Benzothiophene Biphenyls as Inhibitors of Protein Tyrosine Phosphatase 1B with Antihyperglycemic Properties

Michael S. Malamas,* Janet Sredy,[†] Christopher Moxham, Alan Katz, Weixin Xu, Robert McDevitt, Folake O. Adebayo, Diane R. Sawicki,[†] Laura Seestaller, Donald Sullivan, and Joseph R. Taylor

Wyeth-Ayerst Research, Inc., CN 8000, Princeton, New Jersey 08543-8000

Insulin resistance in the liver and peripheral tissues, together with a pancreatic cell defect, are the common causes of Type 2 diabetes. It is now appreciated that insulin resistance can result from a defect in the insulin receptor signaling system, at a site post binding of insulin to its receptor. Protein tyrosine phosphatases (PTPases) have been shown to be negative regulators of the insulin receptor. Inhibition of PTPases may be an effective method in the treatment of Type 2 diabetes. We have identified two novel series of benzofuran/benzothiophene biphenyl oxo-acetic acids and sulfonyl-salicylic acids as potent inhibitors of PTP1B with good oral antihyperglycemic activity. To assist in the design of these inhibitors, crystallographic studies have attempted to identify enzyme inhibitor interactions. Resolution of crystal complexes has suggested that the inhibitors bind to the enzyme active site and are held in place through hydrogen bonding and van der Waals interactions formed within two hydrophobic pockets. In the oxo-acetic acid series, hydrophobic substitutents at position-2 of the benzofuran/benzothiophene biphenyl framework interacted with Phe182 of the catalytic site and were very critical to the intrinsic activity of the molecule. The hydrophobic region of the catalytic-site pocket was exploited and taken advantage by hydrophobic substituents at either the α-carbon or the *ortho* aromatic positions of the oxo-acetic acid moiety. Similar *ortho* aromatic substitutions on the salicylic acid-type inhibitors had no effect, primarily due to the different orientation of these inhibitors in the catalytic site. The most active inhibitors of both series inhibited recombinant human PTP1B with phosphotyrosyl dodecapeptide TRDI(P)YETD(P)Y(P)YRK as the source of the substrate with IC_{50} values in the range of 20−50 nM. Compound **68** was one of the most active compounds in vivo, normalizing plasma glucose levels at the 25 mg/kg dose (po) and the 1 mg/kg dose (ip). Compound **68** was also selective against several other PTPases.

Introduction

Insulin resistance in the liver and peripheral tissues, together with a pancreatic cell defect, are the common causes of Type 2 diabetes.[1] The prevalence of insulin resistance in pre-diabetic or glucose intolerant subjects has long been recognized.[2] The failure of insulin to adequately suppress hepatic glucose output postprandially, combined with the reduced glucose disposal by the peripheral tissues, lead to abnormal glycemic control after feeding. The increased and sustained plasma glucose levels gradually progresses into a number of debilitating diabetic complications: retinopathy, neuropathy, nephropathy, atherosclerosis, and coronary artery disease.[3] Therefore, it is essential to control blood glucose at the early stages of the disease.

Treatment of Type 2 diabetes usually consists of diet, exercise, and hypoglycemic agents. Sulfonylureas are the most widely used antidiabetic agents. These agents act by increasing insulin secretion, but often are ineffective after 5 years of treatment.[4] Recently, a new class of pharmacological agents, the glitazones, have been effectively used as insulin enhancing agents in a large number of insulin resistant patients.[5] Troglitazone, the

first of such a therapeutic agent used for the treatment of Type 2 diabetes, has produced severe liver toxic effects in a small number of patients. Most recently, rosiglitazone, a second member of the glitazone class, has been approved for marketing in the United States, and patients on this new agent will also be monitored for potential liver toxicity. The glitazone-type therapeutic agents are not effective in all Type 2 diabetes patients; therefore, there still remains a great need for more effective and safe agents.

It is now appreciated that insulin resistance is the result of a defect in the insulin receptor signaling system, at a site post binding of insulin to its receptor. Accumulated scientific evidence demonstrating insulin resistance in the major tissues which respond to insulin (muscle, liver, adipose) strongly suggests that the defect in insulin signaling resides at an early step in the signal transduction cascade, specifically at the level of the insulin receptor kinase activity, which appears to be diminished.[6]

Protein tyrosine phosphatases (PTPases) play an important role in the regulation of signal transduction pathways and the phosphorylation of proteins. The interaction of insulin with its receptor leads to the phosphorylation of certain tyrosine molecules (1146, 1150, and 1151) within the receptor protein, thus activating the receptor kinase. PTPases dephosphoryl-

* Wyeth-Ayerst Res., CN 8000, Princeton, NJ 08543-8000. Tel: (732) 274-4428. Fax: (732) 274-4505. E-mail address: malamam@war.wyeth.com.
† Present address: Institute for Diabetes Discovery, 23 Business Park Drive, Branford, CT 06405.

Scheme 1[a]
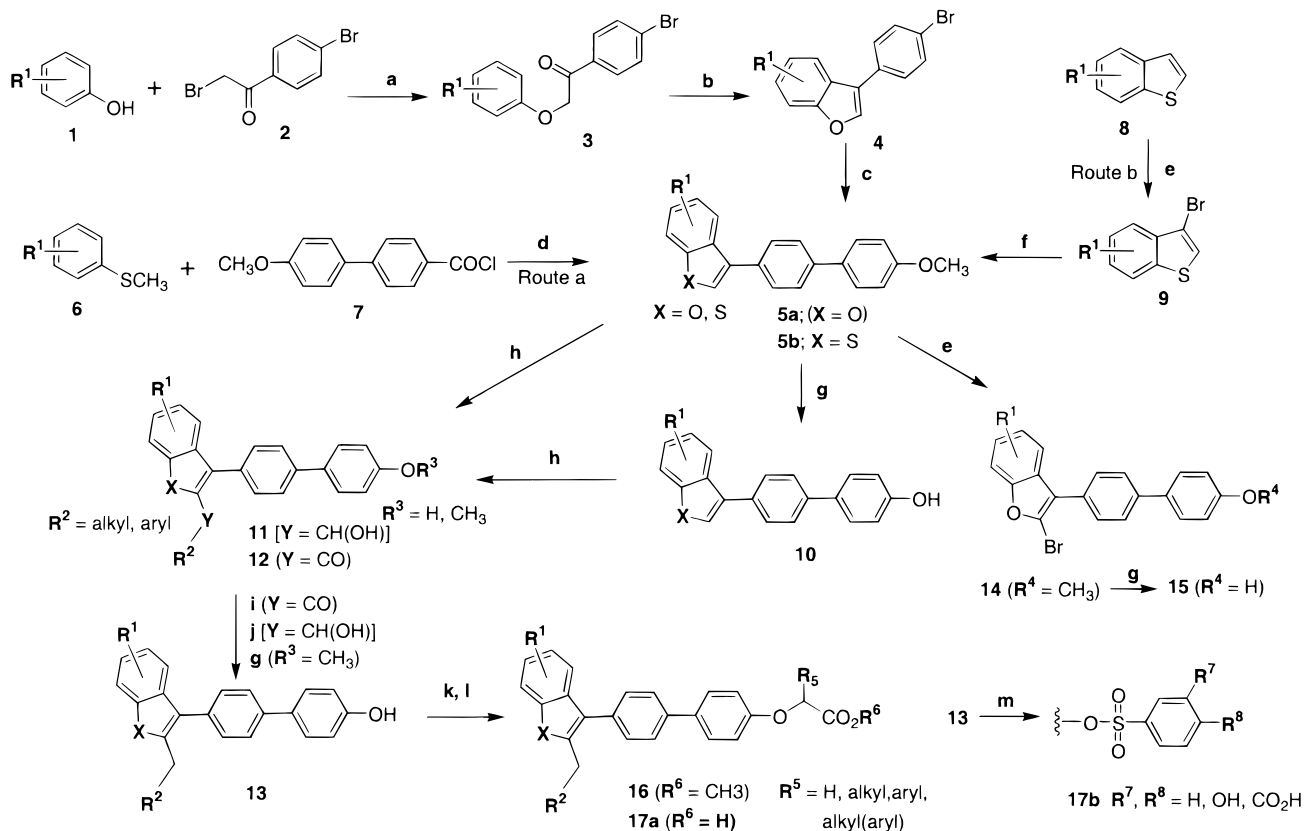
[a] Reagents: (a) K_2CO_3, acetone; (b) H_3PO_4, xylenes; (c) 4-OCH_3-$C_6H_4B(OH)_2$, Pd(PPh$_3$)$_4$, Na$_2$CO$_3$, toluene; (d) n-BuLi, TMEDA, Et$_2$O; (e) Br$_2$, KOAc, AcOH; (f) Pd(OAc)$_2$, K$_2$CO$_3$, 4'-OCH$_3$-biphenyl-4-boronic acid; (g) BBr$_3$, CH$_2$Cl$_2$; (h) R^2-CHO or R^2-CON(CH$_3$)OCH$_3$, n-BuLi, THF; (i) NH$_2$NH$_2$, KOH; (j) NaBH$_4$, TFA; (k) BrCH$_2$CO$_2$CH$_3$, NaH (R^5 = H); HOCH(CHR^5)CO$_2$CH$_3$, PPh$_3$, EtO$_2$CN=NCO$_2$Et [R^5 = alkyl, aryl, alkyl(aryl)]; (l) NaOH, MeOH, THF; (m) ClSO$_2$C$_6$H$_3$R$_7$R$_8$, NaOH, THF.

ate the activated insulin receptor, attenuating the tyrosine kinase activity. PTPases can also modulate post-receptor signaling by catalyzing the dephosphorylation of cellular substrates of the insulin receptor kinase. The enzymes that appear most likely to closely associate with the insulin receptor and, therefore, most likely to regulate the insulin receptor kinase activity, include PTP1B, LAR, PTPα, and SH-PTP2.[7]

McGuire et al.[8] demonstrated that nondiabetic glucose intolerant subjects possessed significantly elevated levels of PTPase activity in muscle tissue vs normal subjects and that insulin infusion failed to suppress PTPase activity as it did in insulin sensitive subjects. Meyerovitch et al.[9] observed significantly increased PTPase activity in the livers of two rodent models of Type 1 diabetes: the genetically diabetic BB rat and the STZ-induced diabetic rat. Sredy et al.[10] observed similar increased PTPase activity in the livers of obese, diabetic ob/ob mice, a genetic rodent model of Type 2 diabetes.

Vanadium containing inhibitors of PTPase have been shown to increase insulin receptor tyrosine phosphorylation, exert insulin-like effects in vitro and in vivo, and decrease hyperglycemia in insulin-deficient animals.[11]

PTP1B, an intracellular nonreceptor PTPase, has been shown to play a major role in the dephosphorylation of the insulin receptor in many cellular and biochemical studies.[12] A recent study with PTP1B knockout mice[13] has also demonstrated that loss of PTP1B activity resulted in an enhancement of the

insulin sensitivity and resistance to weight gain. Potent and orally active PTP1B inhibitors could be potential pharmacological agents for the treatment of Type 2 diabetes and obesity.

In the present study, we are reporting a detailed systematic structure−activity relationship (SAR) study of novel benzofuran/benzothiophene biphenyls as highly potent and orally active PTP1B inhibitors.

Chemistry

The benzofuran and benzothiophene biphenyls described in this paper were prepared according to the synthetic Schemes 1−3. In Scheme 1, alkylation of phenols **1** with 4-bromophenacyl bromide **2** in the presence of potassium carbonate produced ethanones **3**, which upon treatment with polyphosphoric acid at high temperatures (150 °C) afforded benzofurans **4**.[14] Coupling of benzofurans **4** with commercially available boronic acids, using the Suzuki protocol[15] Ph(PPh$_3$)$_4$/Na$_2$CO$_3$, produced benzofuran biphenyls **5a** (X = O). The analogous benzothiophene biphenyls **5b** (X = S) were prepared by two synthetic routes. In route a, thioanisoles **6** were first dilithiated, in the methylthio group and in the *ortho* position of the benzene ring, with 2 equiv of n-butyllithium[16] and, second, treated with equimolecular amounts of 4'-methoxy[1,1'-biphenyl]-4-carbonyl chloride **7** to produce benzothiophene biphenyls **5b** (X = S). In route b, benzothiophenes **8** were first brominated with bromine/potassium acetate to give **9** and, second, treated with 4'-methoxy[1,1'-biphenyl]-4-

Scheme 2[a]
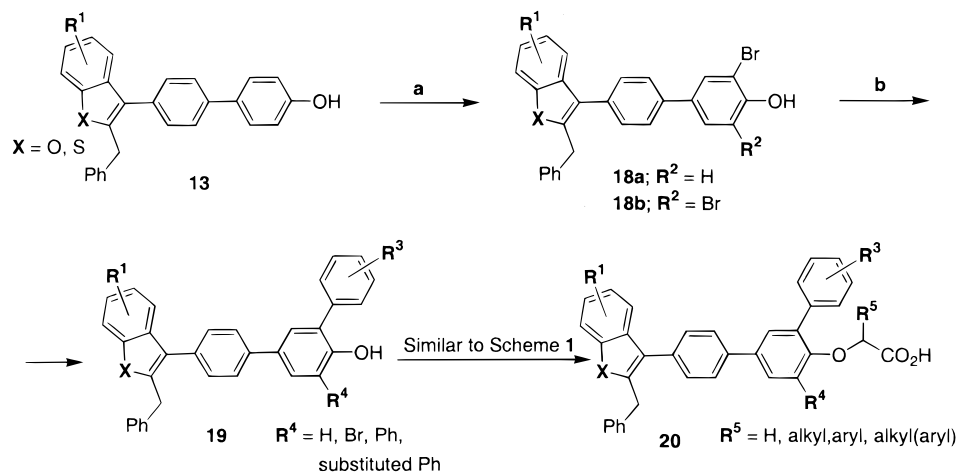
[a] Reagents: (a) Br_2, KOAc, AcOH; (b) aryl-boronic acid, (dppf)$PdCl_2$, K_2CO_3, DME.

Scheme 3[a]
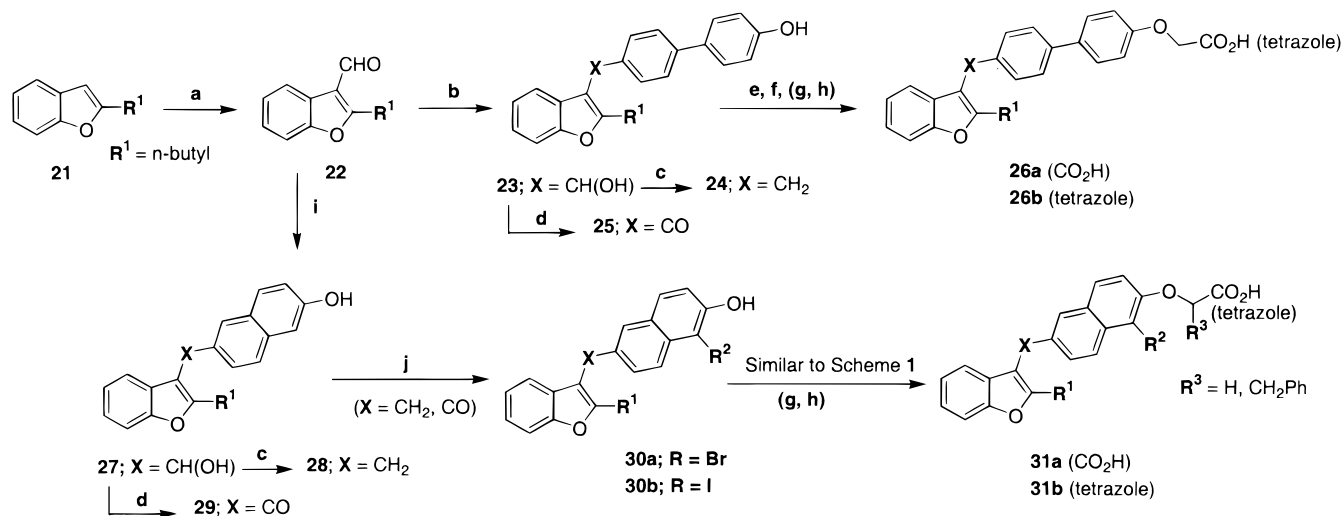
[a] Reagents: (a) DMF, $POCl_3$; (b) *n*-BuLi, 4'-Br-biphenyl-4-ol, THF; (c) Et_3SiH, TFA, CH_2Cl_2; (d) PCC, CH_2Cl_2; (e) $BrCH_2CO_2Me$, NaH, DMF; (f) NaOH, MeOH, THF; (g) $BrCH_2CN$, NaH, DMF; (h) NaN_3, NH_4Cl, DMF; (i) *n*-BuLi, 6-Br-2-naphthol, THF; (j) Br_2, KOAc, AcOH.

ylboronic acid, Ph(PPh$_3$)$_4$, and Na$_2$CO$_3$ to furnish **5b** (X = S). The phenolic compounds **10** were prepared from **5a** and **5b** upon demethylation with boron tribromide. Lithiation of **5a**, **5b**, or **10** first with *n*-BuLi, followed by subsequent addition of alkyl or aromatic aldehydes or the analogous Weinreb amides[17] afforded biphenyls **11** and **12**. Reduction of **11** (R^3 = H) with sodium borohydride/trifluoroacetic acid[18] and that of **12** with hydrazine/KOH[19] produced **13**. When R^3 = CH$_3$ in **11** and **12**, boron tribromide deprotection of the methoxy group was applied after the reduction steps, to furnish **13**. Biphenyls **13** were either alkylated with methyl bromoacetate/NaH or coupled with the required α-hydroxy carboxylates using the Mitsunobu protocol[20] to produce esters **16**. Esters **16** were saponified with sodium hydroxide to produce acids **17a**. The 2-bromobenzofuran biphenyl **15** was prepared from benzofuran **5a** upon bromination with bromine (Br$_2$, KOAc, AcOH) and subsequent demethylation with boron tribromide. The biphenyl-4-yloxysulfonyl benzoic acids **17b** were prepared from biphenyls **13** and the corresponding chlorosulfonyl benzoic acids in the presence of aqueous sodium hydroxide.

In Scheme 2, biphenyls **13** were treated with bromine and potassium acetate at low temperatures (5 °C) under high dilution concentration (0.05 M) to give predominantly the monobromo-biphenyl **18a**. Bromination of **13** with bromine at room temperature gave the dibromo-biphenyl **18b**. Intermediates **18a** and **18b** were coupled with commercially available boronic acids, using the Suzuki protocol [(dppf)PdCl$_2$, K$_2$CO$_3$], to produce ter-phenyls **19**. Intermediates **19** were converted to the acids **20** according to Scheme 1. In Scheme 3, benzofuran **21** was formylated with DMF/POCl$_3$[21] to produce **22**. Treatment of 4'-bromo[1,1'-biphenyl]-4-ol or 6-bromo-2-naphthol with *n*-buyllthium followed by the addition of **22** furnished benzofurans **23** and **27**, respectively. Reduction of **23** and **27** with triethylsilane/trifluroacetic acid[22] afforded **24** and **28**, while oxidation with pyridinium chlorochromate afforded ketones **25** and **29**, respectively. Bromination of **28** and **29** with bromine/potassium acetate furnished naphthalenes **30a** (X = CH$_2$, CO). Intermediates **24**, **25**, and **30a** were converted to the acids **26a** and **31a** according to Scheme 1 and to the tetrazoles **26b** and **31b** by alkylation with bromoac-

Scheme 4[a]

36a; R = CH$_3$
36b; R = (S)-CH(CH$_2$Ph)CO$_2$H
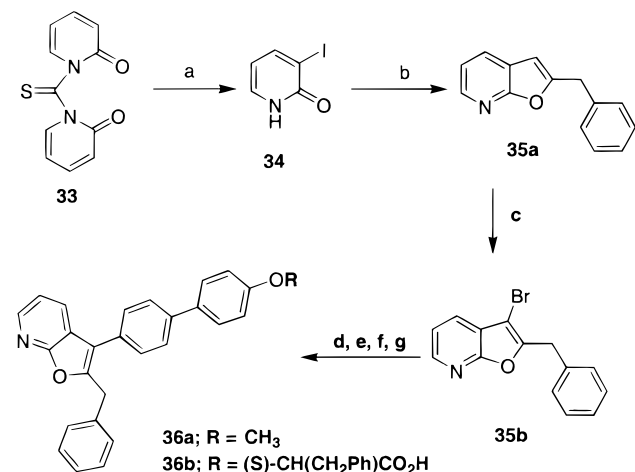
[a] Reagents: (a) I$_2$, Ce(NH$_4$)$_2$(NO$_3$)$_6$, CH$_3$CN; (b) 1-(2-propynyl)benzene, Pd(OAc)$_2$, CuI, *n*-BuNH$_2$; (c) Br$_2$, CCl$_4$; (d) 4′-OCH$_3$-biphenyl-4-B(OH)$_2$, Pd(PPh$_3$)$_4$, Na$_2$CO$_3$, toluene; (e) BBr$_3$, CH$_2$Cl$_2$; (f) (*R*)-(+)-3-phenyllactic acid methyl ester, EtO$_2$CN=NCO$_2$Et, PPh$_3$, benzene; (g) NaOH, MeOH, THF.

etonitrile/NaH and subsequent conversion of the nitriles to tetrazoles with sodium azide and ammonium chloride.

The furo[2,3-*b*]pyridine **36b** was prepared according to Scheme 4. 1,1′-Thiocarbonyldi-2(1*H*)-pyridone **33** was treated with iodine and ammonium cerium nitrate to afford iodo-pyridone **34**.[23] Palladium catalyzed coupling of **34** with 1-(2-propynyl)benzene followed by cyclization in the presence of cuprous iodide and *n*-butylamine furnished furo[2,3-*b*]pyridine **35a**.[24] Intermediate **35a** was first brominated (Br$_2$/CCl$_4$) to **35b** and then converted to the final product **36b** according to Scheme 1.

The imidazole[4,5-*b*]pyridine **45** and benzimidazole **46** were prepared according to Scheme 5. Treatment of pyridine **37** with benzylamine afforded **38**, which was reduced with stannous chloride to amine **39**. Cyclization of **39** with ethyl chloroformate produced imidazo[4,5-*b*]-pyridin-2-one **40**, which was converted to 2-chloro-imidazo[4,5-*b*]pyridine **41** upon treatment with phosphorus oxychloride. The analogous 2-chloro-benzimidazole **43** was prepared from benzimidazole **42** upon alkylation with benzyl bromide. Both intermediates **41** and **43** underwent Suzuki coupling reaction with 4′-methoxy-[1,1′-biphenyl]-4-ylboronic acid in the presence of Pd-(PPh$_3$)$_4$ and sodium carbonate to produce **44** (X = N, C). Intermediates **44** (X = N, C) were converted to the final products **45** and **46** according to Scheme 1.

The oxazole biphenyls (Table 4) were prepared according to synthetic Scheme 6. 1-(4-Bromophenyl)-1-propanone was first converted to oxime **48** (NH$_2$OH/NaOAc), followed by treatment with 4-trifluromethyl-benzoyl chloride and pyridine to produce oxazole **49**.[25] Suzuki coupling of **49** with benzeneboronic acid furnished biphenyl **50a**, which was further converted to the final products **51a** and **51b** according to Schemes **1** and **3**.

Results and Discussion

The test compounds were evaluated for their in vitro inhibitory activity against recombinant human[26] PTP1B with phosphotyrosyl dodecapeptide TRDI(P)YETD(P)Y-(P)YRK (corresponds to the 1142−1153 insulin receptor kinase regulatory domain, phosphorylated on the 1146, 1150, and 1151 tyrosine residues; IR-tri-phosphopeptide) as the source of the substrate.[27] Enzyme reaction progression was monitored via the release of inorganic phosphate as detected by the malachite green-ammonium molybdate method.[28]

The in vitro activity was expressed either as the concentration of the test compound which inhibited enzyme activity by 50% (IC$_{50}$) or the average inhibition of the test compounds at 2.5 and 1 μM concentrations. Samples were prepared in quadruplicates.

The test compounds were evaluated in vivo for their ability to decrease plasma glucose and insulin levels in the genetically obese C57 B1/6J ob/ob diabetic mouse model. The ob/ob animal model is severely insulin resistant, hyperinsulinemic, and glucose intolerant. Insulin resistance in this model has been associated with a reduction in insulin-induced protein tyrosine phosphorylation in tissues such as liver. Also, elevated PTPase activity in the liver of obese ob/ob mice has been observed, which may cause or contribute to the decline in receptor and post-receptor tyrosine phosphorylation.[10] The in vivo activity was assessed at daily doses of 10−100 mg/kg (po) for 4 days and measured as a specified decrease in plasma glucose and insulin levels of the drug-treated group relative to a vehicle-treated control group. Lower doses of 1 mg/kg were evaluated intraperitoneally. A 30−40% (ob/ob) decrease in the plasma glucose level generally normalizes the glucose level to the nondiabetic control level. Ciglitazone was the reference standard in all of the assays.

In the early stage of our discovery program, we have identified that the benzofuran nucleus substituted at position-3 with phenolic moieties exhibited weak inhibitory activity against recombinant rat PTP1B (unpublished results). Modeling studies, using the X-ray crystal structure of h-PTP1B,[29] have suggested that placing the phenolic group of these inhibitors deeper into the catalytic binding pocket (catalytic sequence residues V$_{213}$HCSAGIGR$_{221}$SG) of the enzyme would result in tighter inhibitor−protein interactions: hydrogen bonding interactions of the phenolic hydroxyl group with Arg221. Introduction of the biphenyl-4-ol group at position-3 of the benzofuran ring produced **52** (Table 1), a sub-micromolar inhibitor against h-PTP1B. Masking of the hydroxyl group of **52** resulted in a decrease of the in vitro activity (**52** vs **53**). Substitutions at position-2 of the benzofuran moiety were also crucial to the inhibitory activity. The unsubstituted analogue **54** was inactive at 2.5 μM, while the ethyl analogue **55** was much weaker than **52**. The benzyl and benzoyl analogues **56** and **57** were similar to **52**. The analogous benzothiophene analogues **58** and **59**, however, were quite different. The butyl analogue **58** exhibited inhibitory activity similar to **52**, while the benzyl analogue **59** was much weaker (**59** vs **56**). Introduction of hydroxyl group(s) on the benzyl group (analogues **60**, and **61**) resulted in marked increases of the inhibitory activity (**60**, **61**, vs **59**). Replacement of the phenolic group **52** with an oxo-acetic acid functionality (**62**) resulted in a 3-fold loss of activity. We expected that the acetic acid residue would be closer and bind much tighter to Arg221, via a charge−charge interaction, than the phenolic group of **52**. Modeling studies, however, indicated that the oxo-acetic acid-type inhibitors did not

Scheme 5[a]
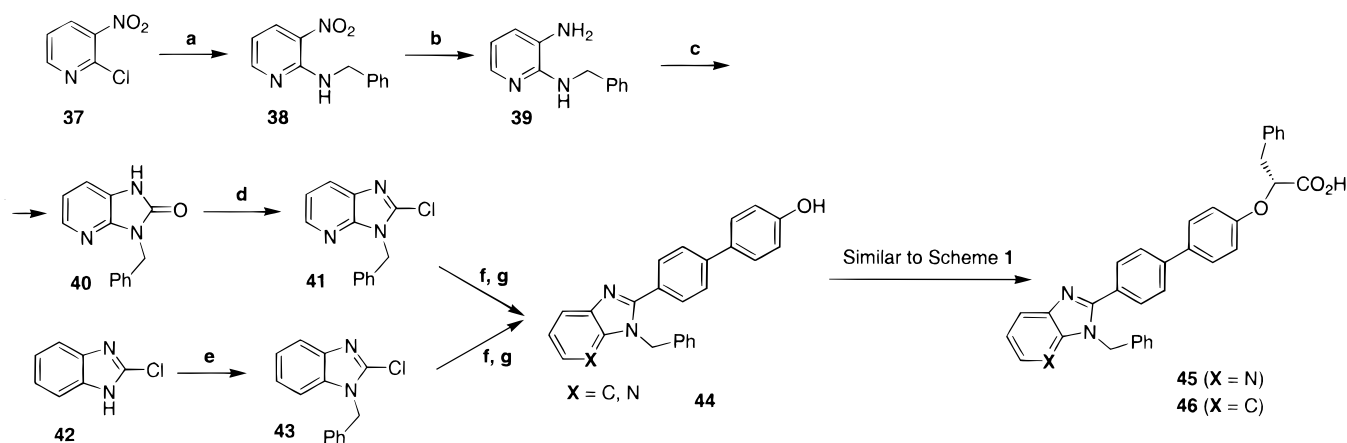
[a] Reagents: (a) $C_6H_5CH_2NH_2$, toluene; (b) $SnCl_2 \cdot 2H_2O$, EtOAc; (c) $ClCO_2Et$, $CHCl_3$; (d) $POCl_3$, PCl_5; (e) $C_6H_5CH_2Br$, NaH, DMF; (f) 4′-OCH_3-biphenyl-4-$B(OH)_2$, $Pd(PPh_3)_4$, Na_2CO_3, toluene; (g) BBr_3, CH_2Cl_2.

Scheme 6[a]
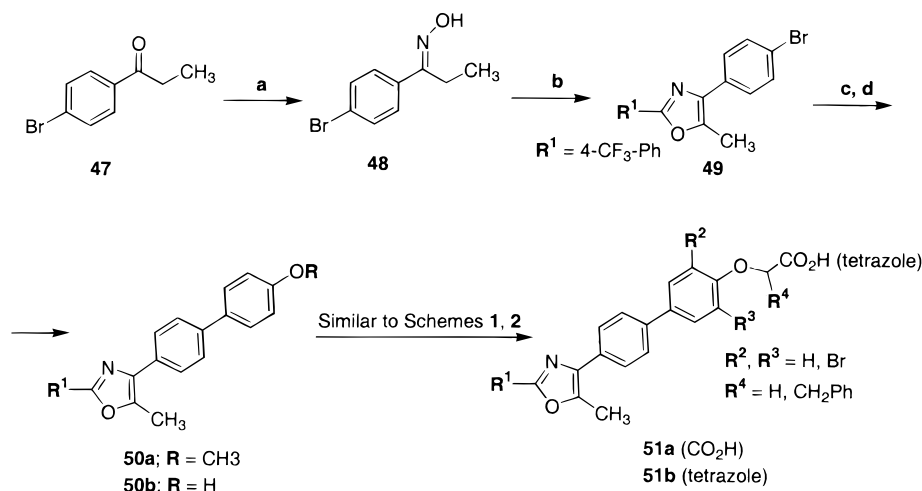
[a] Reagents: (a) NH_2OH, NaOAc, EtOH; (b) 4-CF_3-C_6H_4COCl, pyridine; (c) 4-$OCH_3C_6H_4B(OH)_2$, $Pd(PPh_3)_4$, Na_2CO_3, toluene; (d) BBr_3, CH_2Cl_2.

take advantage of a hydrophobic pocket in the vicinity of Arg221. To test this finding, a phenyllactic moiety replaced the oxo-acetic acid group in **62**. The benzofuran-phenyllactic acid analogue **63** was 5-fold more potent than the acetic acid analogue **62**, with an IC_{50} value of 0.44 μM. Furthermore, we examined the enantioselectivity of the phenyllactic acid-type inhibitors against enzyme inhibition. The *R*- and *S*-enantiomers **67** and **68** were prepared and evaluated against h-PTP1B. Both enantiomers exhibited identical intrinsic activity that was indistinguishable from that of the racemate. Masking of the carboxylate group of **68** as the methyl ester (**70**) was found to be detrimental to the inhibitory activity. Compound **70** was only marginally active at 2.5 μM. Replacement of the phenyllactic group with various aromatic or heteroaromatic groups **71**–**74** produced compounds similar to **68**. The lactic acid analogue **75** was 4-fold weaker than **67**, indicative of the loss of the additional hydrophobic interactions between the inhibitor and enzyme at the vicinity of the catalytic site by eliminating the phenyl group (benzyl changes to methyl) in **75**. The hydroxymethyl analogue **77** was 3-fold better than **67**. Additional hydrogen bonding interactions of the hydroxymethyl group may have contributed to the increased intrinsic activity of

77. Interestingly, the benzoic acid analogue **78** (a combination of the carboxylic acid and phenyl groups of **66**) produced similar results with **66**. Substitutions on the benzofuran portion of the molecule had various effects on the inhibitory activity. The fluoro analogue **90** exhibited a 3-fold increase in inhibitory activity (**90** vs **68**), while the methyl analogue **91** was practically unchanged. The furo-pyridine analogue **92** was 2-fold weaker than **68**, while the benzimidazole analogues **93** and **94** were very weak h-PTP1B inhibitors. The regio-isomeric analogue **95** of **67**, where the biphenyl is attached at position-2 of the benzofuran nucleus, demonstrated similar inhibitory activity to that of **67**.

The benzothiophene analogous compounds were found to be more potent against PTP1B. Both the butyl and benzyl analogues **79** and **80** inhibited h-PTP1B with IC_{50} values of 0.17 and 0.09 μM, respectively. Modifications on the benzyl group, attached at position-2 of the benzothiophene ring, produced inhibitors **82**–**87** with small differences in the their intrinsic activity than the parent compound **80**. Replacement of the benzyl group with either a thiazole **88** or a pyridine **89** moiety resulted in marked loss of the intrinsic activity. Furthermore, truncation of the phenyl portion of the benzothiophene nucleus produced much weaker inhibitors.

Table 1. Chemical and Biological Data of Benzofuran and Benzothiophene Biphenyls[b]
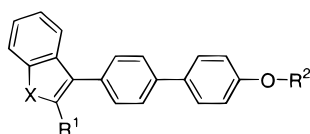
Compd	R[1]	R[2]	X	mp, [0]C	Inhibition of h-PTP1B activity[a] IC$_{50}$ (uM)
52	butyl	H	O	128-129	0.74
53	butyl	CH$_3$	O	85-86	-51 (2.5 uM)
54	H	H	O	174-175	-13 (2.5 uM)
55	ethyl	H	O	128-130	-54 (2.5 uM)
56	benzyl	H	O	151-153	0.92
57	benzoyl	H	O	231-233	0.74
58	butyl	H	S	89-91	0.7
59	benzyl	H	S	178-180	-27 (2.5 uM)
60	4-OH-benzyl	H	S	225-227	1.08
61	2,4-di-OH-benzyl	H	S	199-201	0.58
62	butyl	CH$_2$CO$_2$H	O	126-127	2.19
63	butyl	CH(CH$_2$Ph)CO$_2$H	O	167-170	0.44
64	H	CH(CH$_2$Ph)CO$_2$H	O	142-143	-47 (2.5 uM)
65	Br	CH(CH$_2$Ph)CO$_2$H	O	148-149	-58 (2.5 uM)
66	benzyl	CH(CH$_2$Ph)CO$_2$H	O	164-166	0.27
67	benzyl	CH(CH$_2$Ph)CO$_2$H (R)	O	167-169	0.35
68	benzyl	CH(CH$_2$Ph)CO$_2$H (S)	O	167-168	0.32
69	4-F-benzyl	CH(CH$_2$Ph)CO$_2$H (S)	O	175-176	-38 (0.25 uM)
70	benzyl	CH(CH$_2$Ph)CO$_2$CH$_3$ (S)	O	67-69	-36 (2.5 uM)
71	benzyl	CH(CH2CH$_2$Ph)CO$_2$H (S)	O	152-154	0.22
72	benzyl	CH(CH$_2$CH$_2$-N-phthalinimide)-CO$_2$H (S)	O	182-184	0.34
73	benzyl	CCH$_3$(CH$_2$Ph)CO$_2$H	O	73-75	0.29
74	benzyl	CH(Ph)CO$_2$H (R)	O	177-179	0.4
75	benzyl	CH(CH$_3$)CO$_2$H (R)	O	112-114	1.32
76	benzoyl	CH(CH$_2$Ph)CO$_2$H (R)	O	159-161	0.68
77	CH(OH)phenyl	CH(CH$_2$Ph)CO$_2$H (R)	O	95-97	0.11
78	benzyl	CH$_2$Ph-4-CO$_2$H	O	208-210	0.36
79	butyl	CH(CH$_2$Ph)CO$_2$H (R)	S	159-161	0.17
80	benzyl	CH(CH$_2$Ph)CO$_2$H (R)	S	165-167	0.095
81	butyl	CH(Ph)CO$_2$H (R)	S	157-159	0.11
82	4-F-benzyl	CH(CH$_2$Ph)CO$_2$H (R)	S	151-153	0.12
83	4-OCH$_3$-benzyl	CH(CH$_2$Ph)CO$_2$H (R)	S	75-77	0.077
84	3,4-di-OCH$_3$-benzyl	CH(CH$_2$Ph)CO$_2$H (R)	S	59-61	0.12
85	2,4-di-OCH$_3$-benzyl	CH(CH$_2$Ph)CO$_2$H (R)	S	70-72	0.085
86	2,4-di-OH-benzyl	CH(CH$_2$Ph)CO$_2$H (R)	S	108-110	0.12
87		CH(CH$_2$Ph)CO$_2$H (R)	S	68-70	0.077
88		CH(CH$_2$Ph)CO$_2$H (R)	S	85-87	1.16
89		CH(CH2Ph)CO$_2$H (R)	S	123-125	1.55

Compd	R[1]	R[2]	mp, [0]C	IC$_{50}$ (uM)
90		CH(CH$_2$Ph)CO$_2$H (S)	75-76	0.13
91		CH(CH$_2$Ph)CO$_2$H (R)	63-65	0.41
92		CH(CH$_2$Ph)CO$_2$H (S)	123-125	0.59
93		CH(CH$_2$Ph)CO$_2$H (R)	253-254	-41 (2.5 uM)
94		CH(CH$_2$Ph)CO$_2$H (R)	235-237	-19 (1 uM)

Table 1 (Continued)

Compd	R^1	R^2	mp, ^{0}C	IC_{50} (uM)
95	(benzofuran with Ph)	$CH(CH_2Ph)CO_2H$ (R)	157–159	0.35
96	(thiophene with Ph)	$CH(CH_2Ph)CO2H$ (R)	152–154	0.97
97	(dimethyl thiophene with Ph)	$CH(CH_2Ph)CO2H$ (R)	142–144	0.51

[a] IR-tri-phosphopeptide used as the substrate, and recombinant h-PTP1B as the enzyme. [b] All compounds were prepared according to the synthetic Schemes 1, 4, and 5.
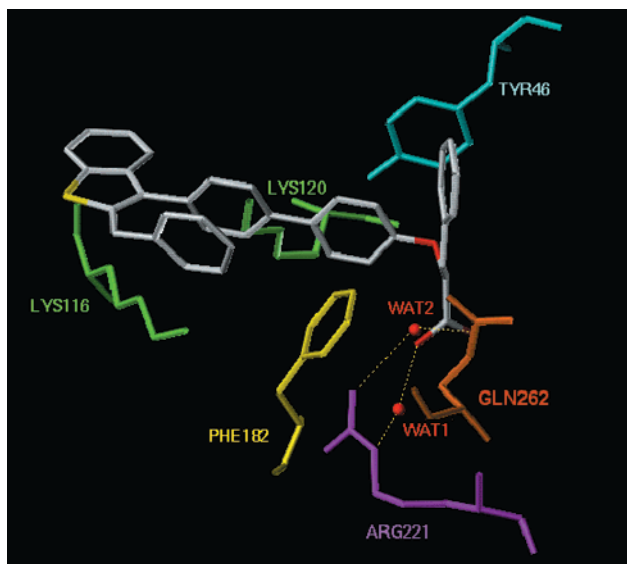

Figure 1. Schematic representation showing compound 80 and its interactions with key residues within the binding catalytic cavity. Key hydrogen bonding interactions between the ligand and the bound waters (WAT1 and WAT2) are shown as yellow dotted lines.
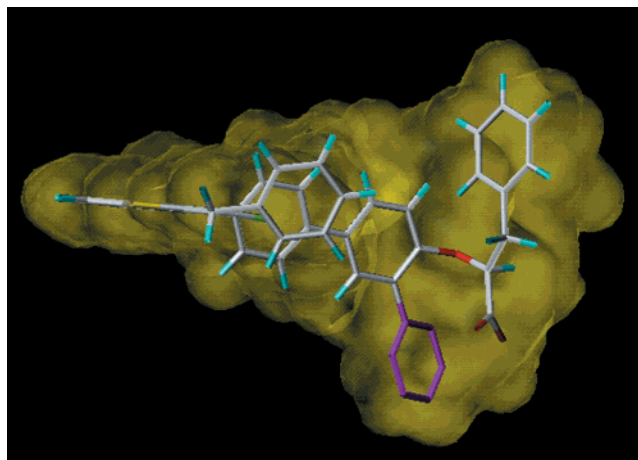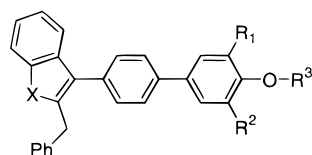

Figure 2. Schematic representation showing compound **80** (with an additional magenta-colored phenyl ring) in the composite volume of the catalytic site. Replacement of the other *ortho* hydrogen with a phenyl ring requires removal of the benzyl side chain from the acetic acid head group.

Both thiophene analogues **96** and **97** were markedly less potent than benzothiophene **80**.

To further improve the intrinsic activity of our compounds, we felt compelled to better understand the inhibitor–protein interactions. Compound **80** was cocrystallized with h-PTP1B, and the crystal structure of the binary complex was refined at 1.85 Å resolution. The bound compound **80** extends deep into the active-site pocket (Figure 1), making several hydrogen bonding and hydrophobic interactions with key residues of the catalytic site. The carboxylic acid portion of the ligand does not interact directly with Arg221 as originally expected, but participates in hydrogen bonds with two water molecules which bridge the ligand with Arg221. Residue Arg221 is responsible for substrate phosphate binding. The phenyl ring of the biphenyl, closest to the carboxylic acid, is sandwiched between residues Tyr46 and Phe182. The A face of the second phenyl of the biphenyl is stacked against Lys120, interacting with its NH_3^+ group. There are several strong van der Waals contacts between the 2-benzyl-benzothiophene tail-portion of the molecule and Lys116. Additionally, the benzyl group interacts with the π face of Phe182.

The complex of compound **80** and PTP1B was further overlapped with several other in-house PTP1B complexes, and the ligands were extracted into separate work areas using the Sybyl software.[30] A composite volume of the ligands was created using the MVOLUME procedure. This volume represents the total volume occupied by all of the ligands determined in house. Figure 2 shows compound **80** (with an additional magenta-colored phenyl ring) in this composite volume. The magenta phenyl ring, added to the position *ortho* to the phenyllactic acid head piece, clearly occupies a hydrophobic region, not reached by our initial inhibitors. Substitution in this position was therefore predicted to contribute to the enhancement of ligand binding affinity.
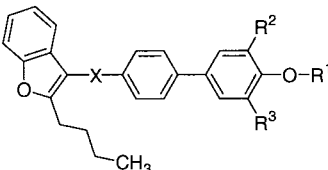
Exploring the findings of the X-ray studies, hydrophobic groups (Table 2) were introduced at the *ortho* position of the phenyllactic acid pharmacophore (terphenyl-type inhibitors). The monobromo analogue **103** was found to be 2-fold better than **80**, and the dibromo analogue **104** was 4-fold better as well with IC_{50} values of 0.058 and 0.025 μM, respectively. Similar increases of the intrinsic activity were also observed for the phenyl-substituted analogues **105** and **106**. Modeling studies (based on the ligand–composite volume overlap, Figure 2) also suggested that an unsubstituted acetic acid moiety instead of the phenyllactic acid might be required for high inhibitory activity, since the terphenyl-type inhibitors (*ortho-ortho*-disubstituted analogues) already take advantage of the hydrophobic pocket at the vicinity of the catalytic site. In agreement with our modeling studies, terphenyl-oxo-acetic acid analogues **112**−**122** were potent h-PTP1B inhibitors with IC_{50} values in the range of 0.025 to 0.1 μM. The *ortho-*

Table 2. Chemical and Biological Data of 2-Benzyl Benzofuran and Benzothiophene Biphenyls[b]

Compd	R^1	R^2	R^3	X	mp, ^{0}C	Inhibition of h-PTP1B activity[a] IC$_{50}$ (uM)
98	Br	H	H	S	54-56	1.07
99	Br	Br	H	S	59-61	0.45
100	I	I	H	S	193-195	0.52
101	Br	H	H	O	110-112	-59 (1uM)
102	Br	Br	H	O	145-146	-43 (1 uM)
103	Br	H	CH(CH$_2$Ph)CO$_2$H (R)	S	81-83	0.058
104	Br	Br	CH(CH$_2$Ph)CO$_2$H (R)	S	87-89	0.025
105	4-OCH$_3$-Ph	H	CH(CH$_2$Ph)CO$_2$H (R)	S	82-84	0.053
106	4-Cl-Ph	H	CH(CH$_2$Ph)CO$_2$H (R)	S	85-87	0.052
107	Br	Br	CH(CH$_2$CH$_2$Ph)CO$_2$H (S)	S	84-86	0.29
108	Br	Br	CH(CH$_2$CH$_2$-N-phthalinimide)-CO$_2$H	S	113-115	0.044
109	Br	Br	CH(CH$_2$CH$_2$NHCOPh-2-CO$_2$H)CO$_2$H	S	130-132	0.18
110	Br	Br	CH(CH$_2$CH2NHCOPh-2-CO$_2$H)CO$_2$CH$_3$	S	95-97	0.054
111	Br	H	CH$_2$CO$_2$H	S	150-152	0.36
112	Br	Br	CH$_2$CO$_2$H	S	183-185	0.10
113	Ph	H	CH$_2$CO$_2$H	S	88-90	0.10
114	4-OCH$_3$-Ph	H	CH$_2$CO$_2$H	S	75-77	0.080
115	4-OC$_2$H$_5$-Ph	H	CH$_2$CO$_2$H	S	98-99	0.052
116	2,3-di-OCH$_3$-Ph	H	CH$_2$CO$_2$H	S	95-97	0.071
117	3,4,5-tri-OCH$_3$-Ph	H	CH$_2$CO$_2$H	S	93-95	0.100
118	4-OCH$_3$-Ph	Br	CH$_2$CO$_2$H	S	94-96	0.029
119	3-OCH$_3$-Ph	Br	CH$_2$CO$_2$H	S	128-130	0.028
120	2,4-di-OCH$_3$-Ph	Br	CH$_2$CO$_2$H	S	103-105	0.047
121	4-OCH$_3$-Ph	4-OCH$_3$-Ph	CH$_2$CO$_2$H	S	99-101	0.025
122	3-OCH$_3$-Ph	3-OCH$_3$-Ph	CH$_2$CO$_2$H	S	83-85	0.025
123	Br	H	CH$_2$CH$_2$CH$_2$CO$_2$H	S	135-137	0.17
124	Br	H	CH(CH$_2$Ph)CO$_2$H (S)	O	80-82	0.056
125	Br	Br	CH(CH$_2$Ph)CO$_2$H (S)	O	90-92	0.038
126	4-OCH$_3$-Ph	H	CH(CH$_2$Ph)CO$_2$H (S)	O	73-75	0.043
127	NO$_2$	H	CH(CH$_2$Ph)CO$_2$H (R)	O	94-95	0.23
128	Br	Br	CH(CH$_2$CH$_3$)CO$_2$H (S)	O	79-80	0.13
129	Br	Br	CH[CH$_2$CH(CH$_3$)$_2$]CO$_2$H (R)	O	81-83	0.054
130	Br	Br	CH[(CH$_2$)$_3$CH$_3$]CO$_2$H	O	75-76	0.052
131	Br	Br	CH[(CH$_2$)$_5$CH$_3$]CO$_2$H	O	72-74	0.023
132	CH3	CH3	CH(CH$_2$Ph)CO$_2$H (R)	O	68-70	0.074
133	cyclopentyl	H	CH(CH$_2$Ph)CO$_2$H (S)	O	73-75	0.055
134	cyclopentyl	H	CH$_2$CO$_2$H	O	164-165	0.17
135	propyl	H	CH(CH$_2$Ph)CO$_2$H (S)	O	90-92	-59 (0.1 uM)
136	NHCH$_2$CO$_2$H	H	CH$_2$CH$_2$Ph	O	159-161	0.082
137	NHCH$_2$CH$_2$CO$_2$H	H	CH$_2$CH$_2$Ph	O	122-124	0.14
138	NHCOCH$_2$CH$_2$CO$_2$H	H	H	O	204-205	0.92
139	NHCOCH=CHCO$_2$H	H	H	O	208-209	0.46
140	NHCO-C$_6$H$_4$-2-CO$_2$H	H	H	O	209-210	0.16

Compd	R^1	R^2	R^3	R^4	mp, ^{0}C	IC$_{50}$ (uM)
141		CH$_2$CO$_2$H	4-OCH$_3$-Ph	4-OCH$_3$-Ph	110-112	0.048
142		CH$_2$CO$_2$H	4-OCH$_3$-Ph	4-OCH$_3$-Ph	125-127	0.031

[a] IR-tri-phosphopeptide used as the substrate, and recombinant h-PTP1B as the enzyme. [b] All compounds were prepared according to the synthetic Schemes 1 and 2.

Table 3. Chemical and Biological Data of 2-Butyl Benzofuran Biphenyls[b]

Compd	R^1	R^2	R^3	X	mp, ^{0}C	Inhibition of h-PTP1B activity[a] IC$_{50}$ (uM)
143	H	H	H	CH$_2$	104-106	1.19
144	H	H	H	CO	38-40	-53 (2.5 uM)
145	H	H	H	CH(OH)	47-49	0.23
146	H	Br	Br	CH(OH)	60-62	1.4
147	CH$_2$CO$_2$H	H	H	CH$_2$	39-40	1.15
148	CH$_2$CO$_2$H	H	H	CH(OH)	111-113	0.54
149	CH$_2$-tetrazole	H	H	CH$_2$	166-168	0.51

[a] IR-tri-phosphopeptide used as the substrate, and recombinant h-PTP1B as the enzyme. [b] All compounds were prepared according to the synthetic Scheme 3.

ortho-disubstituted acetic acids (**118**–**122**) were better than the analogous monosubstituted analogues, since they occupied a larger hydrophobic region at the vicinity of the catalytic site. The second *ortho*-substituent occupies the hydrophobic region previously occupied by the benzyl portion of the phenyllactic head piece (Figure 2). This site is defined on one side by the loop containing residues 215–221 (including Arg221) and on the other by Phe182 and Asp181). These hydrophobic portions of the active site are somewhat larger than the phenyl ring (modeling calculations), further explaining the greater inhibitory activity of the substituted *ortho*-phenyl analogues than the unsubstituted analogues (i.e., **115** vs **113**). Alkoxy groups may also take advantage of favorable hydrogen bond contacts with Arg221. The butyric acid analogue **123** was found to be 2-fold better than the acetic acid analogue **111**. The oxo-butyric acid chain appears to extend deeper into the binding pocket, closer to Arg221, resulting in tighter interactions at the active site.

Similarly, the benzofuran nucleus produced low nanomolar inhibitors (**124**–**135**, **141** and **142**) against h-PTP1B with IC$_{50}$ values in the range of 0.02–0.1 μM. The exception was the nitro and cyclopentyl analogues **127** and **134** which were weaker. Several *N*-carboxylic acid analogues (**136**–**140**), substituted at the *meta*-position of the terminal phenyl group, were also good h-PTP1B inhibitors, with the glycine analogue **136** being the most active (IC$_{50}$ = 0.082 μM).

Introduction of a carbon spacer between the benzofuran and the biphenyl moiety had only a small effect on the inhibitory activity. The methylene-spaced oxo-acetic acid analogue **147** (Table 3) was about 2-fold better than **62**, while the hydroxymethyl-spaced analogue **148** was 4-fold better than **62**. The hydroxylmethyl spacer was also better for the phenolic compound **145** (IC$_{50}$ = 0.2 μM), which was 3-fold better than **52**. The higher inhibitory activity of the hydroxylmethyl-spaced analogues might be the result of additional hydrogen bonding interactions between inhibitor and enzyme. Surprisingly, the *ortho*-substituted dibromo analogue **146** was weaker than **145**. This finding was in contrast to the earlier results with the *ortho*-disubstituted analogues (Table 2), where a marked increase of the

inhibitory activity had been observed. Bioisosteric replacement of the carboxylic acid with a tetrazole moiety produced slightly better h-PTP1B inhibitors (**147** vs **149**).

Replacement of the benzofuran nucleus with a phenyl-substituted oxazole moiety produced several sub-micromolar inhibitors (Table 4). The dibromo-phenyllactic analogue **159** was the best compound of this series with an IC$_{50}$ value of 0.13 μM. Attachment of the oxazole group at regioisomeric positions 4′ or 3′ on the biphenyl nucleus produced similar results (**152** vs **156**).
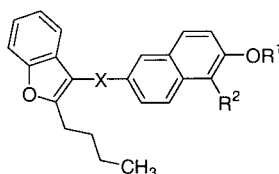
Modeling studies have also suggested that a naphthalene nucleus, substituted at positions 2 and 6, could replace the biphenyl group of our inhibitors. Several compounds were prepared (Table 5) using similar SAR approaches developed in the previous series of h-PTP1B inhibitors. The halogen (bromine, iodine)-substituted phenyllactic acid analogues **167** and **169** were the best compound of this series with IC$_{50}$ values of 0.37 and 0.32 μM, respectively. The analogous oxazole analogue **172** was less active.

The good h-PTP1B inhibitory activity of the benzoic acid analogue **78** (Table 1; IC$_{50}$ = 0.36 μM) served as the starting point for the design of PTP1B inhibitors with similar structural framework and a distinct pharmacophore group. Introduction of a sulfone spacer between the biphenyl central aromatic region and the benzoic acid resulted in a 5-fold improvement of the intrinsic activity (**174** vs **77**; Table 6). The *meta*-substituted analogous compound **175** was only incrementally weaker (IC$_{50}$ = 0.1 μM) than **174**. Addition of a hydroxyl group on the benzoic acid nucleus further improved the inhibitory activity of the compounds. Both salicylic acid analogues **176** and **177** were 2- and 4-fold better than the corresponding benzoic acids **174** and **175**, respectively. Applying similar SAR approaches that were developed for the acetic acid-type inhibitors, we prepared several salicylic acid-type inhibitors (**178**–**185**) with excellent inhibitory activity against h-PTP1B in the low nanomolar range (0.02–0.04 μM). However, the

Table 4. Chemical and Biological Data of Substituted Oxazole Biphenyls[b]
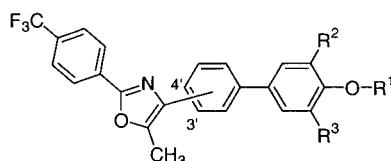
| | | | | | | Inhibition of h-PTP1B activity[a] |
Compd	R^1	R^2	R^3	P.O.A.	mp, ^{0}C	IC$_{50}$ (uM)
150	H	H	H	4'	189-191	-56 (2.5 uM)
151	CH$_2$CO$_2$H	H	H	4'	209-211	0.8
152	CH(CH$_2$Ph)CO$_2$H	H	H	4'	183-184	1.3
153	CH$_2$-tetrazole	H	H	4'	226-227	0.9
154	H	H	H	3'	133-135	-11 (2.5 uM)
155	CH$_2$CO$_2$H	H	H	3'	178-179	-47 (2.5 uM)
156	CH(CH$_2$Ph)CO$_2$H	H	H	3'	148-149	1.6
157	H	Br	Br	4'	79-81	0.65
158	CH$_2$CO$_2$H	Br	Br	4'	165-166	0.47
159	CH(CH$_2$Ph)CO$_2$H	Br	Br	4'	241-243	0.13

^{a} IR-tri-phosphopeptide used as the substrate, and recombinant h-PTP1B as the enzyme. ^{b} All compounds were prepared according to the synthetic Scheme 6.

Table 5. Chemical and Biological Data of 2-Butyl Benzofuran Naphthalenes[b]

| | | | | | Inhibition of h-PTP1B activity[a] |
Compd	R^1	R^2	X	mp, ^{0}C	IC$_{50}$ (uM)
160	H	H	CH$_2$		1.3
161	H	H	CO	55-57	-41 (2.5 uM)
162	H	H	CH(OH)	38-40	1.1
163	H	Br	CH(OH)	48-50	0.48
164	H	Br	CH$_2$		0.33
165	H	I	CH$_2$		0.38
166	CH$_2$CO$_2$H	Br	CH$_2$	122-124	1.4
167	CH(CH$_2$Ph)CO$_2$H	Br	CH$_2$	98-100	0.37
168	CH(CH$_2$Ph)CO$_2$H	Br	CO	165-167	1.2
169	CH(CH$_2$Ph)CO$_2$H	I	CH$_2$	116-118	0.32
170	CH$_2$-tetrazole	Br	CH$_2$	148-150	0.7
171	CH$_2$-tetrazole	Br	CO	160-162	1.1
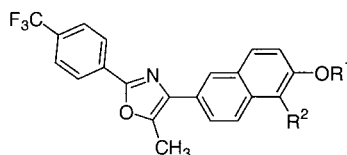
Compd	R^1	R^2	mp, ^{0}C	IC$_{50}$ (uM)
172	CH$_2$CO$_2$H	Br		1.3
173	CH(CH$_2$Ph)CO$_2$H	Br	55-57	-41 (2.5 uM)

^{a} IR-tri-phosphopeptide used as the substrate, and recombinant h-PTP1B as the enzyme. ^{b} All compounds were prepared according to the synthetic Schemes 3 and 6.

findings with the salicylic acid-type inhibitors were in variance to the acetic acid-type inhibitors. While, *ortho*-substitutions in the oxo-acetic acid series had significantly contributed to the enhancement of the inhibitor's intrinsic activity, similar substitutions in the salicylic acid series of compounds (**181**−**183**) had essentially no effect. A different orientation of this class of inhibitors in the active site may play a role in inhibitor−protein interactions and explain these discrepancies. Compound **181**, a member of the salicylic acid-type inhibitors, was

Table 6. Chemical and Biological Data of Sulfono Biphenyls[b]

Compd	R^1	R^2	R^3	R^4	X	mp, ^{0}C	Inhibition of h-PTP1B activity[a] IC$_{50}$ (uM)
174	H	CO_2H	H	H	O	186-188	0.075
175	CO_2H	H	H	H	O	169-171	0.106
176	OH	CO_2H	H	H	O	96-98	0.039
177	CO_2H	OH	H	H	O	171-173	0.026
178	OH	CO_2H	CH_3	CH_3	O	165-167	0.034
179	OH	CO_2H	NO_2	H	O	199-200	0.029
180	OH	CO2H	cyclopentyl	H	O	97-99	0.028
181	OH	CO_2H	H	H	S	236-238	0.028
182	OH	CO_2H	Br	H	S	117-119	0.024
183	OH	CO_2H	Br	Br	S	192-194	0.030

Compd	R^1	R^2	R^3	R^4	R^5	mp, ^{0}C	IC$_{50}$ (uM)
184	OH	CO_2H	H	H		173-175	0.032
185	OH	CO_2H	cyclopentyl	H		105-108	0.040
186	OH	CO_2H	H	H		218-220	0.354
187	OAc	CO_2H	H	H		171-172	1.16
188	OH	CO_2H	NO2	H		105-107	0.178

[a] IR-tri-phosphopeptide used as the substrate, and recombinant h-PTP1B as the enzyme. [b] All compounds were prepared according to the synthetic Schemes 1 and 2.

cocrystallized with h-PTP1B, and the crystal structure of the binary complex was refined at 2.0 Å resolution. This high-resolution structure revealed the binding orientation of the inhibitor in the active site (Figure 3). In contrast to the compound **80** X-ray structure findings, the carboxylic acid of compound **181** makes direct hydrogen bond interactions with the protein at residues Lys120 and Tyr46 and interacts only with one of the two water molecules that interact with Arg221. The aromatic portion of the salicylic acid moiety is sandwiched between residues Tyr46 and Phe182. The lipophilic 2-benzyl-benzothiophene tail-piece of the molecule forms nonspecific van der Waals interactions with the protein. For compound **181**, even though its pharmacophore portion of the molecule (salicylic acid) occupies similar space in the active site as the acetic acid-type inhibitors, the inhibitor orientation is almost opposite to the acetic acid-type inhibitors. *Ortho*-aromatic sub-

stitutents to the sulfonyl-salicylic acid moiety are not accessing the same hydrophobic region as had been previously observed with the similarly substituted acetic acid analogues (Figure 4).

The different orientations of the acetic acid-type (**80**) and the salicylic acid (**181**) ligands in the X-ray crystal structure with PTP1B are shown in Figure 5. Compound **80** was merged with the X-ray crystal structure of compound **181**, and only protein atoms 10 Å from either of the ligands were displayed. A MOLCAD surface[31] was computed for this portion of the protein and was color coded by the lipophilicity of the underlying residues (brown being very lipophilic, blue and green hydrophilic). The acidic pharmacophore portions of the molecules orient to the catalytic site of the protein, while the lipophilic tail-portions of the molecules occupy opposite regions of the protein.
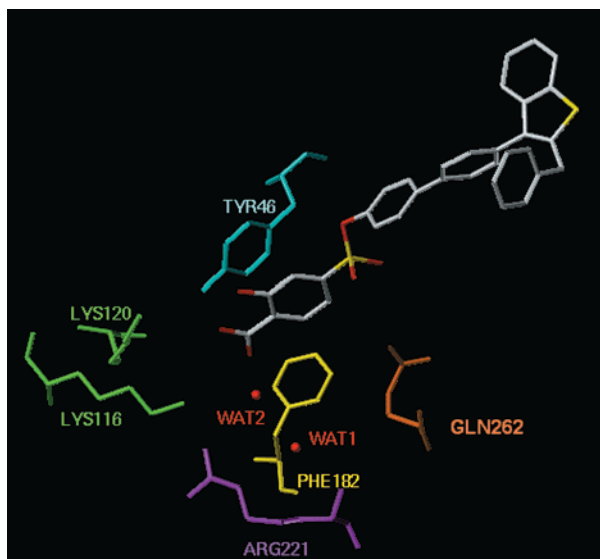
Figure 3. Schematic representation showing compound **181** and its interactions with key residues within the binding catalytic cavity.
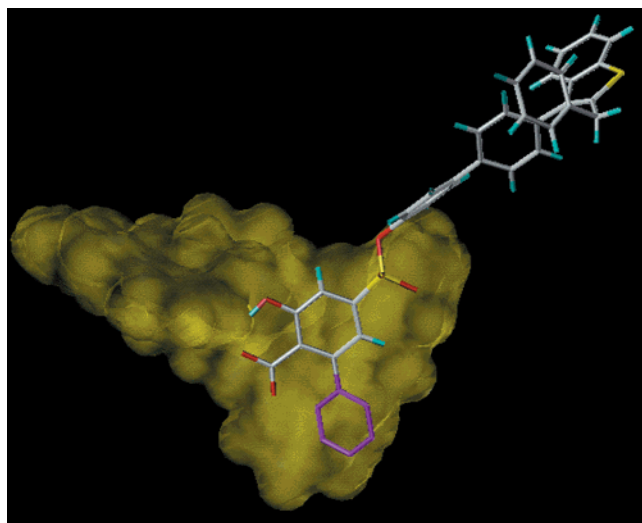

Figure 4. Schematic representation showing compound **181** (with an additional magenta-colored phenyl ring) in the composite volume of the catalytic site. This view highlights the difference in ligand orientation of **181** versus those found for the previously studied ligands.

The compounds were also evaluated in vivo for their ability to decrease plasma glucose and insulin levels in the genetically obese C57 B1/6J ob/ob diabetic mouse model. Initially, the compounds were evaluated at 100 mg/kg dose (po) for 4 days, where the majority among them normalized plasma glucose levels (Table 7). Subsequently, as our compounds had demonstrated anti-hyperglycemic properties and a proof-of-concept had been established, we used lower, 10 and 25 mg/kg, oral doses for in vivo screening. Several compounds significantly decreased plasma glucose levels at the 25 mg/kg dose, while all the compounds tested at 10 mg/kg dose were either marginally active or inactive (data not shown). Compound **68** was one of the most active in vivo compounds, lowering glucose levels by 27% at the oral dose of 25 mg/kg and normalizing glucose levels at the intraperitoneal dose of 1 mg/kg (Table 7). The lower oral potency of **68** may due to the low absorption of the compound. Compound **68** exhibited mean plasma con-
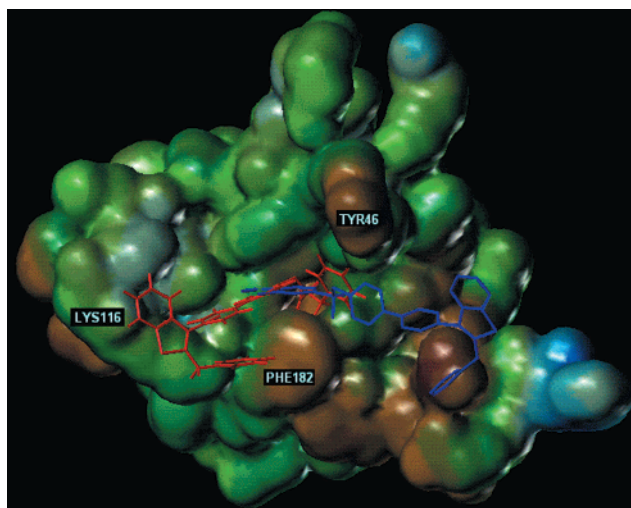

Figure 5. Schematic representation showing compound **80** (red) and **181** (blue) merged with PTP1B (catalytic region) in a MOLCAD surface in which brown represents very lipophilic and blue/green represents hydrophilic environments. Only protein atoms 10 Å from either of the ligands are displayed.

Table 7. In Vivo Data of Selected Compounds

	% decrease in plasma glucose in the ob/ob mouse model	
	mg/kg/day (po)	
Compd	100	25
63	34*,[a]	nt[b]
66	40*	ns[c]
67	35*	ns
68	40*	27*
		37* (1 mg/kg/day; ip)
73	28*	30*
75	39*	ns
77	nt	21*
79	27*	nt
80	37*	nt
81	28*	nt
84	nt	24*
85	nt	24*
86	nt	20*
118	nt	30*
121	nt	26*
131	nt	27*
137	nt	17*
151	40*	nt
152	nt	27*
167	26*	nt
171	25*	nt
176	nt	18*
183	25*	nt
ciglitazone	32*,[d]	nt

[a] Values are percent change relative to vehicle-treated group with use of four to six mice per group; *$p < 0.05$ when compared to vehicle-treated mice. [b] Not tested. [c] NS not significant, generally less than −15% change. [d] Mean of 38 experiments, $p < 0.05$.

centration (AUC$_{0-\infty}$ = 32 μg/mL) after a single 10 mg/kg oral dose in mice, in comparison to a 1 mg/kg intraperitoneal dose, with an AUC$_{0-\infty}$ value of 54 μg/mL. The half-life ($t_{1/2}$) of **68** was found to be 6 to 8 h in mice.

The protein tyrosine phosphatase domains of receptor and nonreceptor PTPases are highly conserved with ~35% mean sequence identity between known phosphatases.[32] Therefore, it is essential that PTP1B inhibitors intended for chronic therapy demonstrate a high level of selectivity. The selectivity of compound **68** was

Table 8. h-PTP1B Specificity of Compound **68**

	IC$_{50}$, nM				
Compd	h-PTP1B[a]	LAR[a]	PTP-a	VH-R	He-PTP
68	322	3250	33700	15900	7100

[a] PTPases implicated in the development of Type 2 diabetes.[7]

evaluated in vitro against several PTPases (Table 8) using the triphosphorylated insulin receptor peptide as the substrate.[7] Compound **68** demonstrated 10 to 100-fold selectivity against the tested PTPases. Compound **68** was least selective (10-fold) over LAR, a PTPase also implicated as a negative regulator of the insulin receptor and development of Type 2 diabetes.

In summary we have identified two novel series of benzofuran/benzothiophene biphenyl oxo-acetic acids and sulfonyl-salicylic acids as potent inhibitors of PTP1B with good oral antihyperglycemic activity. To assist in the design of these inhibitors, crystallographic studies have attempted to identify enzyme inhibitor interactions. Resolution of crystal complexes has suggested that the inhibitors bind to the enzyme active site and are held in place through hydrogen bonding and van der Waals interactions formed within two hydrophobic pockets. In the oxo-acetic acid series, hydrophobic substitutents at position-2 of the benzofuran/benzothiophene biphenyl framework interacted with Phe182 of the catalytic site and were very critical for the intrinsic activity of the molecule. The hydrophobic region of the active-site pocket was exploited and taken advantage of by hydrophobic substituents at either the α-carbon or the *ortho* aromatic positions of the oxo-acetic acid moiety. Similar *ortho* aromatic substitutions on the salicylic acid-type inhibitors had no effect, primarily due to the different orientation of these inhibitors in the catalytic site. The most active inhibitors of both series inhibited recombinant human PTP1B with phosphotyrosyl dodecapeptide TRDI(P)YETD(P)Y(P)YRK as the source of the substrate with IC$_{50}$ values in the range of 20−50 nM. Compound **68** was one of the most active compounds in vivo, normalizing plasma glucose levels at an oral dose of 25 mg/kg (po) and 1 mg/kg (ip). Compound **68** was also selective against several other PTPases.

Experimental Section

Chemistry. Melting points were determined in open capillary tubes on a Thomas-Hoover apparatus and are reported uncorrected. ^{1}H NMR spectra were determined in the cited solvent on a Bruker AM 400 (400 MHz) or a Varian XL-300 (300 MHz) instrument, with tetramethylsilane as an internal standard. Chemical shifts are given in ppm, and coupling constants are in hertz. Splitting patterns are designated as follows: s, singlet; br s, broad singlet; d, doublet; t, triplet; q, quartet; m, multiplet. The infrared spectra were recorded on a Perkin-Elmer 781 spectrophotometer as KBr pellets or as solutions in chloroform. Mass spectra were recorded on either a Finnigan model 8230 or a Hewlett-Packard model 5995A spectrometer. Elemental analyses (C, H, N) were performed on a Perkin-Elmer 240 analyzer, and all compounds are within ±0.4% of theory unless otherwise indicated. Optical rotations were determined in the cited solvent on a Perkin-Elmer model 241 MC polarimeter. All products, unless otherwise noted, were purified by "flash chromatography" with use of 220−400 mesh silica gel. Thin-layer chromatography was done on silica gel 60 F-254 (0.25 mm thickness) plates. Visualization was accomplished with UV light and/or 10% phosphomolybdic acid in ethanol. Unless otherwise noted, all materials were obtained

commercially and used without further purification. All reactions were carried out under an atmosphere of dried nitrogen.

General Procedure for the Synthesis of the Benzofuran and Benzothiophene Biphenyls. All 4,4′-substituted biphenyl compounds were synthesized according to the following representative procedures.

3-(4-Bromophenyl)-1-benzofuran (4, R^1 = H). Potassium carbonate (24.8 g, 179.8 mmol) was added into a mixture of 4-bromophenacyl bromide (50.0 g, 179.8 mmol), phenol (16.9 g, 179.8 mmol), and dry acetone (200 mL). The reaction mixture was refluxed for 12 h, cooled to room temperature, poured into water, and extracted with ethyl ether. The organic extracts were dried over MgSO$_4$. Evaporation gave ω-phenoxy-4-bromoacetophenone as a yellow solid (49.6 g). A mixture of ω-phenoxy-4-bromoacetophenone (49.0 g, 167.8 mmol), polyphosphoric acid (100 g), and xylenes (300 mL) was refluxed for 12 h. The reaction mixture was cooled to room temperature, poured into water, and extracted with ethyl ether. The organic extracts were dried over MgSO$_4$. Evaporation and purification by flash chromatography on silica gel (hexanes/EtAOc 40:1) gave 3-(4-bromophenyl)-1-benzofuran as a yellow solid (36.2 g, 74% yield): mp 70−71 °C; ^{1}H NMR (DMSO-d_6, 400 MHz) δ 7.35−7.4 (m, 2H, Ar-*H*), 7.62−7.7 (m, 5H, Ar-*H*), 7.85−7.9 (m, 1H, Ar-*H*), 8.4 (s, 1H, C*H*); MS *m/e* 272 (M$^+$). Anal. (C$_{14}$H$_9$-BrO) C, H.

3-(4′-Methoxy-biphenyl-4-yl)-benzofuran (5a, R^1 = H, X = O). 4-Methoxy-benzeneboronic acid (14.17 g, 70.5 mmol) in ethyl alcohol (10 mL) was added into a mixture of 3-(4-bromophenyl)-1-benzofuran (17.5 g, 64.1 mmol), sodium carbonate (2 N, 64.1 mL), tetrakis(triphenylphosphine)palladium-(0) (2.23 g, 1.92 mmol), and toluene (200 mL). The reaction mixture was refluxed for 12 h, cooled to room temperature, and treated with hydrogen peroxide (30%, 5 mL) for 1 h. The mixture was poured into water and extracted with ethyl acetate. The organic extracts were dried over MgSO$_4$. Evaporation and crystallization from acetone/ethyl ether gave 3-(4′-methoxy-biphenyl-4-yl)-benzofuran as a white solid (14.9 g, 77% yield): mp 137−138 °C; ^{1}H NMR (DMSO-d_6, 400 MHz) δ 3.79 (S, 3H, OC*H*$_3$), 7.05 (d, *J* = 8.78 Hz, 2H, Ar-*H*), 7.36−7.42 (m, 2H, Ar-*H*), 7.62−7.64 (m, 3H, Ar-H), 7.74 (d, *J* = 8.56 Hz, 2H, Ar-*H*), 7.8 (d, *J* = 8.56 Hz, 2H), Ar-*H*), 7.94−7.98 (m, 1H, Ar-*H*), 8.4 (s, 1H, C*H*); MS *m/e* 300 (M$^+$). Anal. (C$_{21}$H$_{16}$O$_2$) C, H.

4′-Benzofuran-3-yl-biphenyl-4-ol (10, R^1 = H, X = O). Boron tribromide (1.0 M, 6.67 mL, 6.67 mmol) was added dropwise into a cold (−78 °C) mixture of 3-(4′-methoxy-biphenyl-4-yl)-benzofuran (2.0 g, 6.67 mmol) and dichloromethane (25 mL). The reaction mixture was gradually allowed to come to room temperature and stirred for 10 h. The mixture was cooled to 0 °C, and methyl alcohol (5 mL) was added dropwise. After being stirred for 10 min, the mixture was poured into water and extracted with ethyl ether. The organic extracts were dried over MgSO$_4$. Evaporation and crystallization from ethyl ether/hexanes gave 4′-benzofuran-3-yl-biphenyl-4-ol as a yellow solid (1.69 g, 87% yield): mp 174−175 °C; ^{1}H NMR (DMSO-d_6, 400 MHz) δ 6.87 (d, *J* = 8.78 Hz, 2H, Ar-*H*), 7.34−7.41 (m, 2H, Ar-*H*), 7.56 (d, *J* = 8.78 Hz, 2H, Ar-*H*), 7.66 (m, 1H, Ar-*H*), 7.71 (d, *J* = 8.57 Hz, 2H, Ar-*H*), 7.8 (d, *J* = 8.57 Hz, 2H), Ar-*H*), 7.94−7.96 (m, 1H, Ar-*H*), 8.39 (s, 1H, C*H*), 9.58 (S, 1H, O*H*); IR (KBr, cm^{-1}) 3350 (OH); MS *m/e* 286 (M$^+$). Anal. (C$_{20}$H$_{14}$O$_2$) C, H.

[3-(4′-Hydroxy-biphenyl-4-yl)-benzofuran-2-yl]-phenylmethanone (12, R^1, R^3 = H, R^2 = Ph, X = O). *n*-Butyllithium (2.5 N, 8.4 mL, 20.98 mmol) was added dropwise into a cold (−78 °C) mixture of 4′-benzofuran-3-yl-biphenyl-4-ol (3.0 g, 10.49 mmol) and tetrahydrofuran (50 mL). The mixture was gradually allowed to warm to −40 °C and stirred for 3 h. *N*-Methoxy *N*-methyl benzamide (1.6 mL, 10.49 mmol) was added dropwise into the mixture. The new reaction mixture was allowed to warm to 0 °C and stirred for 30 min. The reaction was quenched with aqueous ammonium chloride, poured into water, acidified with HCl (2 N), and extracted with ethyl acetate. The organic extracts were dried over MgSO$_4$.

Evaporation and crystallization from ethyl ether/hexanes gave [3-(4′-hydroxy-biphenyl-4-yl)-benzofuran-2-yl]-phenyl-methanone as a yellow solid (2.9 g, 71% yield): mp 231−232 °C; ^{1}H NMR (DMSO-d_6, 400 MHz) δ 6.87 (d, J = 8.57 Hz, 2H, Ar-H), 7.44−7.46 (m, 3H, Ar-H), 7.51−7.64 (m, 8H, Ar-H), 7.78−7.87 (m, 4H, Ar-H), 9.6 (s, 1H, OH); IR (KBr, cm^{-1}) 3350 (OH), 1650 (CO); MS m/e 390 (M$^+$). Anal. (C$_{27}$H$_{18}$O$_3$) C, H.

4′-(2-Benzyl-benzofuran-3-yl)-biphenyl-4-ol (13, R^1 = H, R^2 = Ph, X = O). Hydrazine monohydrate (1.38 g, 27.68 mmol) was added into a mixture of [3-(4′-hydroxy-biphenyl-4-yl)-benzofuran-2-yl]-phenyl-methanone (2.7 g, 6.92 mmol) and diethylene glycol (20 mL). The reaction mixture was stirred at 180 °C for 1 h. The mixture cooled to room temperature, and potassium hydroxide (1.16 g, 20.76 mmol) was gradually added. The mixture was stirred at 130 °C for 10 h, cooled to room temperature, poured into water, and extracted with ethyl ether. The organic extracts were dried over MgSO$_4$. Evaporation and crystallization from ethyl ether/hexanes/acetone gave 4′-(2-benzyl-benzofuran-3-yl)-biphenyl-4-ol as a white solid (2.45 g, 94% yield): mp 151−153 °C; ^{1}H NMR (DMSO-d_6, 400 MHz) δ 4.26 (s, 2H, CH_2), 6.87 (d, J = 8.78 Hz, 2H, Ar-H), 7.2−7.36 (m, 7H, Ar-H), 7.52−7.62 (m, 6H, Ar-H), 7.75 (d, J = 8.57 Hz, 2H, Ar-H)9.58 (s, 1H, OH); IR (KBr, cm^{-1}) 3360 (OH); MS m/e 376 (M$^+$). Anal. (C$_{27}$H$_{20}$O$_2$) C, H.

(2S)-2-[4′-(2-Benzyl-benzofuran-3-yl)-biphenyl-4-yloxy]-3-phenyl-propionic Acid Methyl Ester (16, R^1 = H, R^2 = Ph, R^5 = CH$_2$Ph, X = O). Diethylazodicarboxylate (1.67 mL, 10.64 mmol) in benzene (20 mL) was added dropwise into a cold (0 °C) mixture of 4′-(2-benzyl-bnzofuran-3-yl)-biphenyl-4-ol (2.0 g, 5.32 mmol), (R)-(+)-3-phenyllactic acid methyl ester (1.91 g, 10.64 mmol), triphenylphosphine (2.8 g, 10.64 mmol), and benzene (50 mL). The reaction mixture was stirred at room temperature for 30 min, poured into water, and extracted with ethyl ether. The organic extracts were dried over MgSO$_4$. Evaporation and purification by flash chromatography on silica gel (hexanes/EtAOc 8:1) gave (2S)-2-[4′-(2-benzyl-benzofuran-3-yl)-biphenyl-4-yloxy]-3-phenyl-propionic acid methyl ester as a yellow oil (2.56 g, 89% yield): ^{1}H NMR (DMSO-d_6, 400 MHz) δ 3.2 (m, 2H, CH_2), 3.65 (s, 3H, CO$_2$CH_3), 4.26 (s, 2H, CH_2), 5.17 (m, 1H, CH), 6.97 (d, J = 8.78, 2H, Ar-H), 7.2−7.37 (m, 12H, Ar-H), 7.57−7.71 (m, 6H, Ar-H), 7.76 (d, J = 8.57, 2H, Ar-H); IR (KBr, cm^{-1}) 1750 (CO); MS m/e 538 (M$^+$). Anal. (C$_{37}$H$_{30}$O$_4$) C, H.

(2S)-2-[4′-(2-Benzyl-benzofuran-3-yl)-biphenyl-4-yloxy]-3-phenyl-propionic Acid (68). Sodium hydroxide (2.5 N, 10 mL) was added into a mixture of (2S)-2-[4′-(2-benzyl-benzofuran-3-yl)-biphenyl-4-yloxy]-3-phenyl-propionic acid methyl ester (2.5 g, 4.65 mmol), methyl alcohol (40 mL), and tetrahydrofuran (40 mL). The reaction mixture was stirred for 1 h, poured into water, acidified with HCl (2 N), and extracted with ethyl ether. The organic extracts were dried over MgSO$_4$. Evaporation and crystallization from ethyl ether/hexanes gave (2S)-2-[4′-(2-benzyl-benzofuran-3-yl)-biphenyl-4-yloxy]-3-phenyl-propionic acid as a white solid (2.32 g, 95% yield): mp 167−169 °C; ^{1}H NMR (DMSO-d_6, 400 MHz) δ 3.2−3.3 (m, 2H, CH_2), 3.65 (s, 3H, CO$_2$CH_3), 4.26 (s, 2H, CH_2), 5.01 (m, 1H, CH), 6.96 (d, J = 8.57, 2H, Ar-H), 7.2−7.38 (m, 12H, Ar-H), 7.57−7.7 (m, 6H, Ar-H), 7.76 (d, J = 8.35, 2H, Ar-H); IR (KBr, cm^{-1}) 3500−2700 (CO$_2$H), 1745 (CO); MS m/e 524 (M$^+$); [α]$^{25}_D$ = −13.4 (1.0, THF). Anal. (C$_{36}$H$_{28}$O$_4$) C, H.

(2S)-2-[4′-(2-Benzyl-benzofuran-3-yl)-biphenyl-4-yloxy]-3-phenyl-propionic Acid Tromethamine Salt (68, Tromethamine Salt). A mixture of (2S)-2-[4′-(2-benzyl-benzofuran-3-yl)-biphenyl-4-yloxy]-3-phenyl-propionic acid (1.0 g, 1.91 mmol), tromethamine (0.23 g, 1.91 mmol), tetrahydrofuran (10 mL), and water (1.0 mL) was stirred at 60 °C for 1 h. The volatiles were removed in vacuo, and the residue was washed with water and dried to give a white solid (1.1 g, 89% yield): mp 147−148 °C; ^{1}H NMR (DMSO-d_6, 400 MHz) δ 3−3.1 (m, 1H, CH_2), 3.2−3.23 (m, 1H, CH_2), 4.26 (s, 2H, CH_2), 4.48 (m, 1H, CH), 6.88 (d, J = 8.78, 2H, Ar-H), 7.17−7.39 (m, 12H, Ar-H), 7.57−7.7 (m, 6H, Ar-H), 7.76 (d, J = 8.35, 2H, Ar-H); MS m/e 523 (M − H)$^+$. Anal. (C$_{36}$H$_{27}$O$_4$·tromethamine·1.5H$_2$O) C, H, N.

(2R)-2-{4′-[2-(Hydroxy-phenyl-methyl)-benzofuran-3-yl]-biphenyl-4-yloxy}-3-phenyl-propionic Acid (74). Sodium borohydride (0.15 g, 4.06 mmol) was added portionwise into a cold (0 °C) mixture of (2R)-2-[4′-(2-benzoyl-benzofuran-3-yl)-biphenyl-4-yloxy]-3-phenyl-propionic acid methyl ester (1.5 g, 2.7 mmol), methyl alcohol (20 mL), and tetrahydrofuran (5 mL). The reaction mixture was allowed to come to room temperature and stirred for 30 min. The mixture was then poured into water, acidified with HCl (2 N), and extracted with ethyl acetate. The organic extracts were dried over MgSO$_4$. Evaporation gave a yellow oil (1.4 g), which was taken in methyl alcohol (20 mL) and tetrahydrofuran (20 mL) and treated with sodium hydroxide (2.5 N, 5.0 mL) for 30 min. The mixture was poured into water, acidified with HCL (2 N), and extracted with ethyl ether. The organic extracts were dried over MgSO$_4$. Evaporation and purification by flash chromatography on silica gel (hexanes/EtAOc 5:1) gave an off-white solid (1.16 g, 79% yield): mp 95−97 °C; ^{1}H NMR (DMSO-d_6, 400 MHz) δ 3.2−3.3 (m, 2H, CH_2), 5.05 (s, 2H, CH_2), 5.4 (m, 1H, CH), 5.9 (s, 1H, OH), 6.96 (m, 2H, Ar-H), 7.2−7.38 (m, 12H, Ar-H), 7.57−7.7 (m, 6H, Ar-H), 7.76 (d, J = 8.35, 2H, Ar-H); IR (KBr, cm^{-1}) 3400−2700 (CO$_2$H), 1740 (CO); MS m/e 539 (M − H)$^+$; Anal. (C$_{36}$H$_{28}$O$_5$) C, H.

3-(4′-Methoxy-biphenyl-4-yl)-benzo[b]thiophene (5b, R^1 = H, X = S). (Route a). n-Butyllithium (99.9 mL, 249.8 mmol) was added dropwise into a cold (−20 °C) mixture of thioanisole (13.98 mL, 119.3 mmol), tetramethylenediamine (18.8 mL, 124.9 mmol), and ethyl ether (300 mL). The mixture was allowed to come to room temperature and stirred for 12 h. Then, the mixture was cooled to −78 °C, and 4′-methoxy-[1,1′-biphenyl]-4-carbonyl chloride (28.0 g, 113.6 mmol) in ethyl ether (50 mL) was added over a 30 min period. The new mixture was stirred at −78 °C for 2 h and then was allowed to come to room temperature and stirred for an additional 20 h. The reaction was quenched with aqueous ammonium chloride, acidified with HCl (2 N), and extracted with ethyl ether. The organic extracts were dried over MgSO$_4$. Evaporation gave a brown oil, which was dissolved in benzene (200 mL). Camphorsulfonic acid (2 g) was added. The mixture was refluxed for 12 h, poured into water, and extracted with ethyl acetate. The organic extracts were dried over MgSO$_4$. Evaporation and crystallization of the residue from ethyl ether/acetone gave 3-(4′-methoxy-biphenyl-4-yl)-benzo[b]thiophene as an off-white solid (7.8 g, 23% yield): mp 134−136 °C; ^{1}H NMR (DMSO-d_6, 400 MHz) δ 3.8 (s, 3H, OCH_3), 7.06 (d, J = 8.78 Hz, 2H, Ar-H), 7.4−7.42 (m, 2H, Ar-H), 7.64−7.67 (m, 4H, Ar-H), 7.77 (d, J = 8.35 Hz, 2H, Ar-H), 7.85 (s, 1H, CH), 7.94 (m, 1H, Ar-H), 8.09 (m, 1H, Ar-H); MS m/e 316 (M$^+$). Anal. (C$_{21}$H$_{16}$OS) C, H.

(Route b). Palladium(II) acetate (2.9 mg, 0.01 mmol) was added into a mixture of 3-bromo-benzo[b]-thiophene (1.4 g, 6.58 mmol), 4′-methoxy-biphenyl-4-boronic acid (1.5 g, 6.58 mmol), potassium carbonate (2.27 g, 16.45 mmol), acetone (20 mL), and H$_2$O (20 mL). The reaction mixture was stirred at 65 °C for 2 h, poured into water, and extracted with ethyl acetate. The organic extracts were dried over MgSO$_4$. Evaporation and crystallization from ethyl ether/hexanes gave 3-(4′-methoxy-biphenyl-4-yl)-benzo[b]thiophene as an off-white solid (1.76 g, 85% yield).

4′-(2-Benzyl-benzo[b]thiophen-3-yl)-3-bromo-biphenyl-4-ol; 4′-(2-Benzyl-benzo[b]thiophen-3-yl)-3,5-dibromo-biphenyl-4-ol [18a R^2 = H, 18b (R^2 = Br), R^1 = H, X = O]. Bromine (1.47 mL, 28.7 mmol) in acetic acid (50 mL) was added dropwise over a 30 min period into a cold (5 °C) mixture of 4′-(2-benzyl-benzo[b]thiophen-3-yl)-biphenyl-4-ol (7.5 g, 19.1 mmol), potassium acetate (18.6 g, 190.1 mmol), and acetic acid (300 mL). After the addition, the mixture was stirred for 10 min, poured into water, and extracted with ethyl ether. The organic extracts were washed with aqueous sodium bisulfite and dried over MgSO$_4$. Evaporation and purification by flash chromatography on silica gel (hexanes/EtAOc/CH$_2$Cl$_2$ 3:1:1) gave 4′-(2-benzyl-benzo[b]thiophen-3-yl)-3-bromo-biphenyl-4-ol as a light yellow solid (4.7 g): mp 54−56 °C; ^{1}H NMR (DMSO-d_6, 400 MHz) δ 4.22 (s, 2H, CH_2), 7.09 (s, 1H, 8.35 (1H, Ar-H), 7.2−7.24 (m, 3H, Ar-H), 7.3−7.4 (m, 4H, Ar-H),

7.5−7.56 (m, 3H, Ar-*H*), 7.6 (dd, *J* = 8.57, 2.42, 1H, Ar-*H*), 7.8 (d, *J* = 8.57 Hz, 2H, Ar-*H*), 7.88 (d, *J* = 2.42 Hz, 1H, Ar-*H*), 7.93 (m, 1H, Ar-*H*), 10.45 (s, 1H, O*H*); IR (KBr, cm^{-1}) 3440 (OH); MS *m/e* 477 (M$^+$). Anal. (C$_{27}$H$_{19}$BrOS) C, H. 4′-(2-Benzyl-benzo[*b*]thiophen-3-yl)-3,5-dibromo-biphenyl-4-ol was also obtained as a light yellow solid (1.4 g): mp 59−61 °C; ^{1}H NMR (DMSO-*d*$_6$, 400 MHz) *δ* 4.21 (s, 2H, C*H*$_2$), 7.18−7.22 (m, 3H, Ar-*H*), 7.3−7.4 (m, 4H, Ar-*H*), 7.45 (m, 1H, Ar-*H*), 7.52 (d, *J* = 8.35 Hz, 2H, Ar-*H*), 7.84 (d, *J* = 8.35 (, 2H, Ar-*H*), 7.91−7.93 (m, 1H, Ar-*H*), 7.94 (S, 2H, Ar-*H*), 10.12 (s, 1H, O*H*); IR (KBr, cm^{-1}) 3470 (OH); MS *m/e* 548(M$^+$). Anal. (C$_{27}$H$_{18}$Br$_2$OS) C, H.

4,4″-Dimethoxy-5′-{4-[2-(phenylmethyl)benzo[*b*]thien-3-yl]phenyl}-[1,1′;3′,1″-terphenyl]-2′-ol (19, R^1 = H, R^3 = OCH$_3$, R^4 = 4-OCH$_3$-Ph, X = O). Palladium(II) acetate (81 mg, 0.036 mmol) was added into a mixture of 4′-(2-benzyl-benzo[*b*]thiophen-3-yl)-3,5-dibromo-biphenyl-4-ol (1.0 g, 1.82 mmol), 4-methoxy-benzeneboronic acid, barium hydroxide (0.93 g, 5.46 mmol), 1,2-dimethoxyethane (10 mL), and water (10 mL). The mixture was stirred at 75 °C for 10 h, poured into water, and extracted with ethyl ether. The organic extracts were dried over MgSO$_4$. Evaporation and purification by flash chromatography on silica gel (hexanes/EtAOc 4:1) gave 4,4″-dimethoxy-5′-{4-[2-(phenylmethyl)benzo[*b*]thien-3-yl]phenyl}[1,1′;3′,1″-terphenyl]-2′-ol as a yellow solid (0.45 g, 41% yield): mp 80−82 °C; ^{1}H NMR (DMSO-*d*$_6$, 400 MHz) *δ* 3.82 (s, 6H, OC*H*$_3$, OC*H*$_3$), 4.23 (s, 2H, C*H*$_2$), 7.04 (d, *J* = 8.78 Hz, 4H, Ar-*H*), 7.2−7.24 (m, 3H, Ar-*H*), 7.3−7.4 (m, 4H, Ar-*H*), 7.5−7.56 (m, 5H, Ar-*H*), 7.61 (d, *J* = 8.78 Hz, 2H, Ar-*H*), 7.9−7.97 (m, 3H, Ar-*H*), 8.32 (s, 1H, O*H*); IR (KBr, cm^{-1}) 3420 (OH); MS *m/e* 604 (M$^+$). Anal. (C$_{41}$H$_{32}$O$_3$S) C, H.

[(4,4″-Dimethoxy-5′-{2-(phenylmethyl)benzo[*b*]thien-3-yl]phenyl]-[1,1′;3′,1″-terphenyl]-2′-yl)oxy]-acetic Acid (121). Methyl bromoacetate (0.16 mL, 1.66 mmol) was added dropwise into a mixture of 4,4″-dimethoxy-5′-{4-[2-(phenyl-methyl)benzo[*b*]thien-3-yl]phenyl}[1,1′;3′,1″-terphenyl]-2′-ol (1.0 g, 1.66 mmol), potassium carbonate (0.23 g, 1.66 mmol), and *N,N*-dimethylformamide (10 mL). The reaction mixture was stirred at 75 °C for 2 h, poured into water, and extracted with ethyl acetate. The organic extracts were dried over MgSO$_4$. Evaporation and purification by flash chromatography on silica gel (hexanes/EtAOc 4:1) gave a yellow oil (1.05 g). The crude product was taken in methyl alcohol (10 mL) and tetrahydro-furan (10 mL) and treated with NaOH (2.5 N 3.0 mL) for 30 min. Then, the reaction mixture was poured into water, acidified with HCl (2 N), and extracted with ethyl ether. The organic extracts were dried over MgSO$_4$. Evaporation and purification by flash chromatography on silica gel (hexanes/EtAOc 3:1) gave [(4,4″-mimethoxy-5′-{2-(phenylmethyl)benzo-[*b*]thien-3-yl]phenyl}-[1,1′;3′,1″-terphenyl]-2′-yl)oxy]-acetic acid as a white solid (0.79 g, 72% yield): mp 99−101 °C; ^{1}H NMR (DMSO-*d*$_6$, 400 MHz) *δ* 3.82 (s, 8H, OC*H*$_3$, OC*H*$_3$, C*H*$_2$), 4.23 (s, 2H, C*H*$_2$), 7.04 (d, *J* = 8.78 Hz, 4H, Ar-*H*), 7.2−7.24 (m, 3H, Ar-*H*), 7.3−7.4 (m, 4H, Ar-*H*), 7.5−7.56 (m, 3H, Ar-*H*), 7.62−7.68 (m, 6H, Ar-*H*), 7.9−7.97 (m, 3H, Ar-*H*), 12.6 (brs, 1H, CO$_2$*H*); IR (KBr, cm^{-1}) 3400−2700 (CO$_2$H), 1740 (CO); MS *m/e* 662 (M$^+$). Anal. (C$_{43}$H$_{34}$O$_5$S) C, H.

Benzyl-(3-nitro-pyridin-2-yl)-amine (38). To a stirred solution of 2-chloro-3-nitropyridine (10 g, 63.1 mmol) in toluene (100 mL) was added in one portion benzylamine (13.5 g, 126 mmol), and the mixture refluxed overnight. The mixture was cooled to room temperature and filtered. The solvent was evaporated, and the residue was purified by flash chromatog-raphy (EtOAc/petroleum ether 1/10) to give benzyl-(3-nitro-pyridin-2-yl)-amine as a yellow solid: mp 78 °C; ^{1}H NMR (DMSO-*d*$_6$, 400 MHz) *δ* 4.8 (d, *J* = 5.93 Hz, 2H, C*H*$_2$), 6.78 (m, 1H, Ar-*H*), 7.2−7.23 (m, 1H, Ar-*H*), 7.3−7.4 (m, 4H, Ar-*H*), 8.44 (m, 2H, Ar-*H*), 8.95 (t, *J* = 6.93 Hz, 1H, N*H*); IR (KBr, cm^{-1}) 3400 (NH); MS *m/e* 229 (M$^+$). Anal. (C$_{12}$H$_{11}$N$_3$O$_2$) C, H, N.

Benzyl-pyridine-2,3-diamine (39). A solution of benzyl-(3-nitro-pyridin-2-yl)-amine (5 g, 21.8 mmol) and tin(II) chlo-ride dihydrate (24.6 g, 109.1 mmol) in EtOAc (100 mL) was refluxed for 2 h. The reaction mixture was cooled to room temperature, quenched with saturated aqueous NaHCO$_3$ (until

basic), diluted with EtOAc (350 mL), stirred overnight, and filtered. The biphasic filtrate was separated, and the aqueous phase was extracted with ethyl acetate. The combined organic extracts were dried over MgSO$_4$. Evaporation and purification by flash chromatography on silica gel (EtOAc/petroleum ether, 1/1) gave benzyl-pyridine-2,3-diamine as a light red solid: mp 88 °C; ^{1}H NMR (DMSO-*d*$_6$, 400 MHz) *δ* 4.55 (d, *J* = 5.93 Hz, 2H, C*H*$_2$), 4.73 (brs, 2H, N*H*$_2$), 6.02 (t, *J* = 5.93 Hz, 1H, N*H*), 6.35 (m, 1H, Ar-*H*), 6.67 (m, 1H, Ar-*H*), 7.2 (m, 1H, Ar-h), 7.23−7.33 (m, 5H, Ar-H); IR (KBr, cm^{-1}) 3400 (NH); MS *m/e* 200 (M+H)$^+$. Anal. (C$_{12}$H$_{13}$N$_3$) C, H, N.

3-Benzyl-1,3-dihydro-imadazo[4,5-*b*]pyridin-2-one (40). Ethyl chloroformate (3.34 g, 30.7 mmol) was added to a solution of benzyl-pyridine-2,3-diamine (2.78 g, 14.0 mmol) in chloroform (70 mL), and the mixture was refluxed for 1.5 h. The reaction mixture was washed with aqueous NaHCO$_3$ and water, and evaporated to dryness. The residue was purified by flash chromatography on silica gel (EtOAc/chloroform, 1/1) to give a brown oil, which was dissolved in absolute ethanol (15 mL) and added to a solution of sodium ethoxide (10 mmol) in absolute ethanol (15 mL). The mixture was refluxed for 3 h and concentrated in vacuo, and the residue was diluted with water, neutralized with HCl (2 N), and extracted with ethyl acetate. The extracts were washed with water and dried over MgSO$_4$. Evaporation and purification by flash chroma-tography (EtOAc/petroleum ether, 1/3) gave 3-benzyl-1,3-dihydro-imadazo[4,5-*b*]pyridin-2-one as an orange solid: mp 172 °C; ^{1}H NMR (DMSO-*d*$_6$, 400 MHz) *δ* 5.02 (s, 2H, CH2), 7.02 (m, 1H, Ar-H), 7.25 (m, 1H, Ar-H), 7.33 (m, 5H, Ar-H), 7.94 (m, 1H, Ar-H), 11.2 (brs, 1H, NH); IR (KBr, cm^{-1}) 1710 (CO); MS *m/e* 225 (M + H)$^+$. Anal. (C$_{13}$H$_{11}$N$_3$O) C, H, N.

3-Benzyl-2-(4′-methoxy-biphenyl-4-yl)-3*H*-imadazo[4,5-*b*]pyridine (44, X = N). Phosphorus pentachloride (0.92 g, 4.44 mmol) was added into a refluxing suspension of 3-benzyl-1,3-dihydro-imadazo[4,5-*b*]pyridin-2-one (1.0 g, 4.44 mmol) in phosporus oxychloride (15 mL). The mixture was refluxed for 12 h. The solvent was then removed in vacuo, and the residue was treated with water and basified with sodium hydroxide (5 N) under external cooling. The solution was extracted with ethyl acetate, washed with brine, and dried over MgSO$_4$. Evaporation and purification by flash chromatography (EtOAc/petroleum ether 1/3) gave a yellow solid (423 mg). The haloimidazopyridine (0.423 g, 1.74 mmol) and tetrakis(tri-phenylphosphine)palladium(0) (100 mg, 0.09 mmol) were dissolved in the 1,2-dimethoxyethane (5 mL) and stirred at room temperature for 10 min. 4′-methoxy-biphenyl-4-boronic acid (0.61 g, 1.91 mmol) was then added, followed by aqueous sodium carbonate (2 M, 3.5 mL). The mixture was refluxed for 12 h, diluted with water, and extracted with dichlo-romethane. The organic extracts were dried over MgSO$_4$. Evaporation and purification by flash chromatography (EtOAc/dichloromethane 1/10) gave 3-benzyl-2-(4′-methoxy-biphenyl-4-yl)-3*H*-imadazo[4,5-b]pyridine as a white solid: mp 159 °C; ^{1}H NMR (DMSO-*d*$_6$, 400 MHz) *δ* 3.81 (s, 3H, OC*H*$_3$), 5.69 (s, 2H, C*H*$_2$), 7.02 (m, 4H, Ar-*H*), 7.21−7.26 (m, 3H, Ar-*H*), 7.46 (m, 1H, Ar-*H*), 7.7−7.8 (m, 7H, Ar-*H*), 8.5 (d, *J* = 6.15 Hz, 1H, Ar-*H*); MS *m/e* 391 (M + H)$^+$. Anal. (C$_{26}$H$_{21}$N$_3$O) C, H, N.

2-Benzylfuro[2,3-*b*]pyridine (35a). Iodine (7.6 g, 69.3 mmol) in acetonitrile (300 mL) was added dropwise into a suspension of 1,1-thiocarbonyldi-2(1*H*)-pyridone (16.6 g, 69.3 mmol), ammonium cerium(IV) nitrate (28.5 g, 51.97 mmol) and acetonitrile (700 mL). The reaction mixture was stirred at 50 °C for 24 h and concentrated to give a brown solid. The residue was partitioned in ethyl acetate and cold (0 °C) aqueous sodium bisulfite. The aqueous phase was recovered and extracted twice with ethyl acetate. The combined organic extracts were washed with water and brine and dried over MgSO$_4$. Evaporation and purification by flash chromatography (dichloromethane/isopropyl alcohol 20/1) gave 3-iodo-2-pyri-done as a yellow solid (2.1 g). A mixture of 3-iodo-2-pyridone (1.2 g, 5.43 mmol), palladium acetate (12 mg), triphenylphos-phine (24 mg), copper(I) iodide (24 mg), *n*-butylamine (1.08 mL, 10.86 mmol), 3-phenyl-1-propyne (0.83 mL, 6.5 mmol), and tetrahydrofuran (9 mL) was stirred at 55 °C for 48 h. The

reaction was quenched with water and extracted with ethyl acetate. The organic extracts were dried over $MgSO_4$. Evaporation and purification by flash chromatography (hexanes/ethyl acetate 4/1) gave 2-benzylfuro[2,3-*b*]pyridine as a brown oil (0.74 g, 65% yield): ^{1}H NMR (DMSO-d_6, 400 MHz) δ 4.13 (s, 2H, CH2), 6.33 (s, 1H, CH), 7.15 (m, 1H, Ar-H), 7.26 (m, 1H, Ar-H), 7.28 (m, 4H, Ar-H), 7.78 (dd, $J = 7.5$, 1.54 Hz, 1H, Ar-H), 8.22 (dd, $J = 6.6$, 1.76 Hz, 1H, Ar-H); MS m/e 209 (M[+]). Anal. ($C_{14}H_{11}NO$) C, H, N.

2-Benzyl-3-(4′-methoxy[1,1′-biphenyl]-4-yl)furo[2,3-*b*]pyridine (36a). Bromine (1.6 mL, 31.7 mmol) was added dropwise into mixture of 2-benzylfuro[2,3-*b*]pyridine (1.57 g, 31.7 mmol), sodium acetate (5.2 g, 63.4 mmol), and acetic acid over a 50 min period. The mixture was stirred for 6 h, poured into water, and extracted with dichloromethane. The organic extracts were washed with NaOH (0.01 N), water, and brine and dried over $MgSO_4$. Evaporation and purification by flash chromatography on silica gel (hexanes/ethyl acetate 9/1) gave 3-bromo-2-benzylfuro[2,3-*b*]pyridine as a yellow solid (0.8 g). The product was dissolved in acetone (7 mL) and added into a mixture of 4′-methoxy-biphenyl-4-boronic acid (0.69 g, 3.06 mmol), potassium carbonate (0.96 g, 6.95 mmol), palladium acetate (2.5 mg), and water 7 (mL). The reaction was stirred at 65 °C for 24 h, poured into water, and extracted with dichloromethane. The organic extracts were dried over $MgSO_4$. Evaporation and purification by flash chromatography (hexanes/ethyl acetate 9/1) gave 2-benzyl-3-(4′-methoxy[1,1′-biphenyl]-4-yl)furo[2,3-*b*]pyridine as an off-white solid (0.26 g, 24% yield): ^{1}H NMR (DMSO-d_6, 400 MHz) δ 3.87 (s, 3H, OCH₃), 4.27 (s, 2H, CH₂), 7.03 (d, $J = 8.78$ Hz, 2H, Ar-H), 7.24 (m, 2H, Ar-H), 7.33 (m, 4H, Ar-H), 7.55 (8.56 Hz, 1H, Ar-H), 7.61 (d, $J = 7.56$ Hz, 2H, Ar-H), 7.69 (d, $J = 8.78$ Hz, 2H, Ar-H), 7.78 (dd, $J = 7.5$, 1.54 Hz, 1H, Ar-H), 8.22 (dd, $J = 6.6$, 1.76 Hz, 1H, Ar-H); MS m/e 391 (M[+]). Anal. ($C_{27}H_{21}NO_2$) C, H, N.

4′-(2-Benzyl-benzofuran-3-yl)-3-nitro-biphenyl-4-ol. Iron-(III) nitrate nonahydrate (8.04 g, 19.9 mmol) was added to a solution of 4′-(2-benzyl-benzofuran-3-yl)-biphenyl-4-ol (6.8 g, 18.1 mmol) in absolute ethanol (80 mL), and the mixture was stirred at 45 °C for 1.5 h. The reaction mixture was cooled to room temperature, poured into HCl (0.1 N), and extracted with ethyl acetate. The extracts were washed with brine and dried over $MgSO_4$. Evaporation and purification by flash chromatography on silica gel (EtOAc/petroleum ether 1/10) gave 4′-(2-benzyl-benzofuran-3-yl)-3-nitro-biphenyl-4-ol as a yellow solid: mp 75 °C; ^{1}H NMR (DMSO-d_6, 400 MHz) δ 4.26 (s, 2H, CH₂), 7.2–7.36 (m, 8H, Ar-H), 7.6–7.64 (m, 4H, Ar-H); 7.8 (d, $J = 8.35$ Hz, 2H, Ar-H), 7.9 (dd, $J = 8.78$, 2.41 Hz, 2H, Ar-H), 8.2 (d, $J = 2.63$ Hz, 1H, Ar-H)11.16 (brs, 1H, OH); IR (KBr, cm[−1]) 3350 (OH); MS m/e 420 (M − H)[+]. Anal. ($C_{27}H_{19}NO_4$·0.5H_2O) C, H, N.

1-(4-Bromo-phenyl)-propanone Oxime (48). Sodium acetate (80.0 g, 0.97 mol) was added into a mixture of 1-(4-bromo-phenyl)-propanone (52.0 g, 0.24 mol), hydroxylamine hydrochloride (50.8 g, 0.73 mol), ethyl alcohol (500 mL), and water (100 mL). The reaction mixture was stirred at 60 °C for 1 h, poured into water, and extracted with ethyl ether. The organic extracts were dried over $MgSO_4$. Evaporation and crystallization from ethyl ether/ hexanes gave 1-(4-bromo-phenyl)-propanone oxime as a white solid (49.6 g, 89% yield): ^{1}H NMR (DMSO-d_6, 400 MHz) δ 1.0 (t, $J = 7.69$ Hz, 3H, CH₃), 2.67 (q, $J = 7.69$ Hz, 2H, CH₂), 7.5 (m, 4H, Ar-H), 11.2 (s, H, OH), IR (KBr, cm[−1]) 3200 (OH); MS m/e 227 (M[+]). Anal. (C_9H_{10}BrNO) C, H, N.

4-(4-Bromo-phenyl)-5-methyl-2-(4-trifluoromethyl-phenyl)-oxazole (49). Pyridine (3.55 mL, 43.86 mmol) was added into a mixture of 1-(4-bromo-phenyl)-propanone oxime (10.0 g, 43.86 mmol) and toluene (20 mL). The reaction mixture was stirred for 30 min, and 4-trifluoromethyl-phenyl acetyl chloride (16.27 mL, 109.6 mmol) was added dropwise. The mixture was stirred at 100 °C for 24 h, poured into water, and extracted with ethyl acetate. The organic extracts were dried over $MgSO_4$. Evaporation and purification by flash chromatography on silica gel (hexanes/EtOAc 40:1) gave 4-(4-bromo-phenyl)-5-methyl-2-(4-trifluoromethyl-phenyl)-oxazole as a white solid

(7.3 g, 43% yield): mp 82−84 °C; ^{1}H NMR (DMSO-d_6, 400 MHz) δ 2.63 (s, 3H, CH₃), 7.58 (m, 4H, Ar-H), 7.9 (d, $J = 8.35$ Hz, 2H, Ar-H), 8.18 (d, $J = 8.35$ Hz, 2H, Ar-H); MS m/e 381 (M[+]). Anal. ($C_{17}H_{11}BrF_3NO$) C, H, N.

4-(4′-Methoxy-biphenyl-4-yl)-5-methyl-2-(4-trifluoromethyl-phenyl)-oxazole (50a, R[1] = 4-CF₃-Ph). 4-Methoxy-benzeneboronic acid (1.44 g, 7.19 mmol) in ethyl alcohol (5 mL) was added into a mixture of 4-(4-bromo-phenyl)-5-methyl-2-(4-trifluoromethyl-phenyl)-oxazole (2.5 g, 6.54 mmol), sodium carbonate (2 N, 6.5 mL), tetrakis(triphenylphosphine)palladium-(0) (0.23 g, 0.196 mmol), and toluene (200 mL). The reaction mixture was refluxed for 12 h, cooled to room temperature, and treated with hydrogen peroxide (30%, 5 mL) for 1 h. The mixture was poured into water and extracted with ethyl acetate. The organic extracts were dried over $MgSO_4$. Evaporation and crystallization from hexanes/ethyl ether gave 4-(4′-methoxy-biphenyl-4-yl)-5-methyl-2-(4-trifluoromethyl-phenyl)-oxazole as a white solid (2.2 g, 82% yield): mp 167−168 °C; ^{1}H NMR (DMSO-d_6, 400 MHz) δ 2.68 (s, 3H, CH₃), 3.8 (s, 3H, OCH₃), 7.05 (d, $J = 8.78$ Hz, 2H, Ar-H), 7.65 (d, $J = 8.78$ Hz, 2H, Ar-H), 7.68 (d, $J = 8.57$ Hz, 2H, Ar-H), 7.73 (d, $J = 7.57$ Hz, 2H, Ar-H), 7.9 (d, $J = 8.35$ Hz, 2H, Ar-H), 8.2 (d, $J = 8.35$ Hz, 2H, Ar-H); MS m/e 409 (M[+]). Anal. ($C_{24}H_{18}F_3NO_2$) C, H, N.

6-[(2-Butyl-benzofuran-3-yl)-hydroxy-methyl-naphthalen-2-ol (27, R[1] = butyl). *n*-Butyllithium (17.9 mL) was added dropwise into a cold (−78 °C) mixture of 6-bromo-2-naphthol (5.0 g, 22.42 mmol), and tetrahydrofuran (100 mL). The reaction mixture was stirred for 2 h, and then 2-butyl-benzofuran-3-carboxaldehyde (4.53 g, 22.42 mmol) in tetrahydrofuran (5 mL) was added dropwise. The mixture was stirred for 30 min, quenched with aqueous ammonium chloride, poured into water, acidified with HCl (2 N), and extracted with ethyl ether. The organic extracts were dried over $MgSO_4$. Evaporation and purification by flash chromatography on silica gel (hexanes/EtOAcc 3:1) gave 6-[(2-butyl-benzofuran-3-yl)-hydroxy-methyl-naphthalen-2-ol as a yellow solid (6.8 g): mp 38−40 °C; ^{1}H NMR (DMSO-d_6, 400 MHz) δ 0.88 (t, $J = 7.25$ Hz, 3H, CH₃), 1.38−1.4 (m, 2H, CH₂), 1.6−1.64 (m, 2H, CH₂), 1.9 (t, $J = 7.47$ Hz, 2H, CH₂), 7.03−7.05 (m, 3N, Ar-H), 7.12 (m, 1H, Ar-H), 7.36 (dd, $J = 8.57$, 1.76 Hz, 1H, Ar-H), 7.41 (8.13 Hz, 2H, Ar-H), 7.59 (d, $J = 8.57$ Hz, 1H, Ar-H), 7.75 (d, $J = 7.69$ (1H, Ar-H), 7.9 (s, 1H, Ar-H), 9.64 (s, 1H, OH); IR (KBr, cm[−1]) 3370 (OH); MS m/e 346 (M[+]). Anal. ($C_{23}H_{22}O_3$) C, H.

6-[(2-Butyl-benzofuran-3-ylmethyl)-naphthalen-2-ol (28, R[1] = butyl). Triethylsilane (7.4 mL, 46.38 mmol) was added into a cold (0 °C) mixture of 6-[(2-butyl-benzofuran-3-yl)-hydroxy-methyl-naphthalen-2-ol (8.0 g, 23.19 mmol) and dichloromethane (100 mL). After 10 min, trifluoroacetic acid (10 mL) was added into the reaction mixture, and the reaction was stirred for 30 min, poured into water, and extracted with ethyl ether. The organic extracts were dried over $MgSO_4$. Evaporation gave 6-[(2-butyl-benzofuran-3-ylmethyl)-naphthalen-2-ol as a brown oil (6.2 g): ^{1}H NMR (DMSO-d_6, 400 MHz) δ 0.85 (t, $J = 7.25$ Hz, 3H, CH₃), 1.15−1.5 (m, 2H, CH₂), 1.6−1.63 (m, 2H, CH₂), 2.81 (t, $J = 7.47$ Hz, 2H, CH₂), 4.07 (s, 2H, CH₂), 7.0−7.05 (m, 3H, Ar-H), 7.17 (t, $J = 7.25$ Hz, 1H, Ar-H), 7.34 (d, $J = 7.7$ Hz, 1H, Ar-H), 7.45 (d, $J = 8.13$ Hz, 1H, Ar-H), 7.57 (d, $J = 8.56$ Hz, 1H, Ar-H), 7.62 (m, 2H, Ar-H), 9.6 (s, 1H, OH); IR (KBr, cm[−1]) 3400 (OH); MS m/e 330 (M[+]). Anal. ($C_{23}H_{22}O_2$) C, H.

1-Bromo-6-(2-butyl-benzofuran-3-ylmethyl)-naphthalen-2-ol (30a, R[1] = Butyl, X = CH₂). Bromine (0.96 mL, 18.78 mmol) in acetic acid (10 mL) was added dropwise over a 30 min period into a cold (5 °C) mixture of 6-[(2-butyl-benzofuran-3-ylmethyl)-naphthalen-2-ol (6.2 g, 18.78 mmol) and acetic acid (50 mL). After the addition, the mixture was poured into water and extracted with ethyl ether. The organic extracts were washed with aqueous sodium bisulfite and dried over $MgSO_4$. Evaporation gave 1-bromo-6-(2-butyl-benzofuran-3-ylmethyl)-naphthalen-2-ol as a brown oil (5.6 g): mp 54−56 °C; ^{1}H NMR (DMSO-d_6, 400 MHz) δ 0.85 (t, $J = 7.25$ Hz, 3H, CH₃), 1.2−1.35 (m, 2H, CH₂), 1.6−1.65 (m, 2H, CH₂), 2.83 (t, $J = 7.47$

Hz, 2H, C*H₂*), 4.1 (s, 2H, C*H₂*), 7.04 (t, *J* = 7.69 Hz, 1H, Ar-H), 7.13 (t, *J* = 7.25 Hz, 1H, Ar-H), 7.23 (d, *J* = 8.78 Hz, 1H, Ar-H), 7.3 (d, *J* = 7.67 Hz, 1H, Ar-H), 7.42 (m, 2H, Ar-H), 7.67 (m, 2H, Ar-H), 7.89 (d, 8.18 Hz, 1H, Ar-H), 10.42 (s, 1H, OH); IR (KBr, cm⁻¹) 3480 (OH); MS *m/e* 408 (M⁺). Anal. (C₂₇H₁₁-BrO2) C, H.

5-[1-Bromo-6-(2-butyl-benzofuran-3-ylmethyl)-naphthalen-2-yloxy]-1*H*-tetrazole (170). Sodium hydride (0.16 g, 3.96 mmol) was added into a mixture of 1-bromo-6-(2-butyl-benzofuran-3-ylmethyl)-naphthalen-2-ol (1.35 g, 3.3 mmol) and *N,N*-dimethylformamide (10 mL). The mixture was stirred for 1 h, and bromoacetonitrile (0.27 mL, 3.96 mmol) was added dropwise. The mixture was stirred for 1 h, poured into water, acidified with HCl (2 N), and extracted with ethyl ether. Evaporation gave a yellow oil (1.15 g). The residue was taken in *N,N*-dimethylformamide (20 mL) and treated with sodium azide (1.29 g, 19.8 mmol), and ammonium chloride (1.05 g, 19.8 mmol). The mixture was stirred at 120 °C for 10 h, poured into water, acidified with HCl (2 N), and extracted with ethyl ether. The organic extracts were dried over MgSO₄. Evaporation and purification by flash chromatography on acidic silica gel (hexanes/EtOAc 2:1) gave 5-[1-bromo-6-(2-butyl-benzofuran-3-ylmethyl)-naphthalen-2-yloxy]-1*H*-tetrazole as a white solid (0.98 g): mp 148−150 °C; ¹H NMR (DMSO-*d₆*, 400 MHz) δ 0.85 (t, *J* = 7.25 Hz, 3H, C*H₃*), 1.2−1.35 (m, 2H, C*H₂*), 1.6−1.65 (m, 2H, C*H₂*), 2.83 (t, *J* = 7.47 Hz, 2H, C*H₂*), 4.16 (s, 2H, C*H₂*), 5.66 (s, 2H, C*H₂*), 7.06 (t, *J* = 7.69 Hz, 1H, Ar-*H*), 7.13 (t, *J* = 7.25 Hz, 1H, Ar-*H*), 7.32 (d, *J* = 7.67 Hz, 1H, Ar-*H*), 7.44 (d, *J* = 8.78 Hz, 1H, Ar-*H*), 7.51 (d, *J* = 8.78 Hz, 1H, Ar-*H*), 7.57 (d, *J* = 8.78 Hz, 2H, Ar-*H*), 7.8 (s, 1H, Ar-*H*), 7.92 (d, *J* = 8.78 Hz, 1H Ar-*H*), 7.98 (d, *J* = 8.78 Hz, 1H, Ar-*H*); MS *m/e* 490 (M⁺). Anal. (C₂₅H₂₃BrN₄O₂) C, H, N.

(2-Butyl-benzofuran-3-yl)-(4′-hydroxy-biphenyl-4-yl)-methanone (25, R¹ = Butyl). Pyridinium chlorochromate (1.74 g, 8.06 mmol), was added into a mixture of 4′-[(2-butyl-benzofuran-3-yl)-hydroxy-methyl]-biphenyl-4-ol (2.0 g, 5.37 mmol) and dichloromethane (20 mL). The reaction mixture was stirred for 1 h, diluted with ethyl ether, and filtered through a florisil pad. The organic extracts were dried over MgSO4. Evaporation and purification by flash chromatography on silica gel (hexanes/EtOAc 3:1) gave (2-butyl-benzofuran-3-yl)-(4′-hydroxy-biphenyl-4-yl)-methanone as a yellow solid (1.1 g): ¹H NMR (DMSO-*d₆*, 400 MHz) δ 0.73 (t, *J* = 7.25 Hz, 3H, C*H₃*), 1.14−1.18 (m, 2H, C*H₂*), 1.62−1.69 (m, 2H, C*H₂*), 2.78 (t, *J* = 7.47 Hz, 2H, C*H₂*), 7.21 (t, *J* = 7.87 Hz, 1H, Ar-*H*), 7.35−7.4 (m, 3H, Ar-*H*), 7.66 (d, *J* = 8.13 Hz, 1H, Ar-*H*), 7.95−8.02 (m, 2H, Ar-*H*), 8.14 (d, *J* = 8.78 1H, Ar-*H*), 8.34 (s, 1H, Ar-*H*), 11.05 (s, 1H, O*H*); IR (KBr, cm⁻¹) 3200 (OH), 1600 (CO); MS *m/e* 370 (M⁺). Anal. (C₂₃H₂₂O₃) C, H.

6-(2-Butyl-benzofuran-3-ylmethyl)-1-iodo-naphthalen-2-ol (30b, R¹ = Butyl, X = CH₂). Iodine (1.16 g, 4.55 mmol) was added portionwise into a cold (0 °C) mixture of 6-[(2-butyl-benzofuran-3-ylmethyl)-naphthalen-2-ol (1.5 g, 4.55 mmol), sodium hydroxide (0.35 g, 9.1 mmol), and methyl alcohol (20 mL). The reaction mixture was stirred for 3 h, poured into water, acidified with HCl (2 N), and extracted with ethyl acetate. The organic extracts were dried over MgSO₄. Evaporation and purification by flash chromatography on silica gel (hexanes/EtOAc 2:1) gave 6-(2-butyl-benzofuran-3-ylmethyl)-1-iodo-naphthalen-2-ol as a brown oil (1.85 g): ¹H NMR (DMSO-*d₆*, 400 MHz) δ 0.86 (t, *J* = 7.25 Hz, 3H, C*H₃*), 1.3−1.35 (m, 2H, C*H₂*), 1.6−1.67 (m, 2H, C*H₂*), 2.85 (t, *J* = 7.47 Hz, 2H, C*H₂*), 4.1 (s, 2H, C*H₂*), 7.05 (t, *J* = 7.69 Hz, 1H, Ar-*H*), 7.14−7.18 (m, 2H, Ar-*H*), 7.31 (d, *J* = 7.67 Hz, 1H, Ar-*H*), 7.39 (d, *J* = 8.56 Hz, 1H, Ar-*H*), 7.42 (d, *J* = 8.13 Hz, 1H, Ar-*H*), 7.63 (s, 1H, Ar-*H*), 7.67 (d, *J* = 8.57 Hz, 1H, Ar-*H*), 7.84 (d, *J* = 8.78 Hz, 1H, Ar-*H*), 10.54 (s, 1H, O*H*); IR (KBr, cm⁻¹) 3450 (OH); MS *m/e* 476 (M⁺). Anal. (C₂₃H₂₁IO₂) C, H.

4-[4′-(2-Benzyl-benzofuran-3-yl)-biphenyl-4-yloxysulfonyl]-2-hydroxy-benzoic Acid (175). Sodium hydroxide (50%) was added dropwise into cold (0 °C) mixture of 4′-(2-benzyl-benzofuran-3-yl)-biphenyl-4-ol (1.0 g, 2.66 mmol), 4-chlorosulfonyl-2-hydroxy-benzoic acid (1.25 g, 5.32 mmol), and tetrahydrofuran (50 mL) in a rate that the reaction was maintained at pH 11. The reaction was stirred for 30 min, poured into water, acidified with HCl (2 N), and extracted with ethyl ether. The organic extracts were dried over MgSO₄. Evaporation and purification by flash chromatography on acidic silica gel (hexanes/EtAOc 2:1) gave 4-[4′-(2-benzyl-benzofuran-3-yl)-biphenyl-4-yloxysulfonyl]-2-hydroxy-benzoic acid as a white solid, (0.67 g, 43% yield): mp 96−98 °C; ¹H NMR (DMSO-*d₆*, 400 MHz) δ 4.26 (s, 2H, C*H₂*), 7.18−7.39 (m, 11H, Ar-*H*), 7.6−7.64 (m, 4H, Ar-*H*), 7.77−7.82 (m, 4H, Ar-*H*), 7.99 (d, *J* = 8.56 Hz, 1H, Ar-*H*); IR (KBr, cm⁻¹) 3420 (OH), 3600−2700 (CO₂H); MS *m/e* 575 (M − H)⁺. Anal. (C₃₄H₂₄O₇S·0.5·H₂O) C, H.

Inhibition of Triphosphorylated Insulin Receptor Dodecaphosphopeptide Dephosphorylation by h-PTP1B. Preparation of Recombinant h-PTP1B. Human recombinant PTP1B (321 aa form) was prepared as described.[26]

Measurement of PTPase Activity. The malachite green-ammonium molybdate method, as described by Lanzetta et al.[28] and adapted for the plate reader, was used for the nanomolar detection of liberated phosphate by recombinant h-PTP1B. The assay used, as substrate, a dodecaphosphopeptide custom synthesized by AnaSpec, Inc. (San Jose, CA). The peptide, TRDIYETDYYRK, corresponding to the 1142−1153 catalytic domain of the insulin receptor, is phosphorylated on tyrosine residues 1146, 1150, and 1151. The recombinant h-PTP1B was diluted with buffer, pH 7.4, containing 33 mM Tris-HCl, 2 mM EDTA, and 50 mM β-mercaptoethanol to obtain an approximate activity of 1000−2000 nmol/min/mg protein. The diluted enzyme was preincubated for 10 min at 37 °C with or without test compound and 81.83 mM HEPES reaction buffer, pH 7.4. Peptide substrate, at a final concentration of 50 μM, was equilibrated to 37 °C in a LABLINE Multi-Blok heater. The preincubated recombinant enzyme preparation with or without drug was added to initiate the dephosphorylation reaction, which proceeded at 37 °C for 30 min. The reaction was terminated by the addition the malachite green-ammonium molybdate-Tween 20 stopping reagent (MG/AM/Tw). The stopping reagent consisted of 3 parts 0.45% malachite green hydrochloride, 1 part 4.2% ammonium molybdate tetrahydrate in 4 N HCl, and 0.5% Tween 20. Sample blanks were prepared by the addition of MG/AM/Tw to substrate and of the preincubated recombinant enzyme with or without drug. The color was allowed to develop at room temperature for 30 min, and the sample absorbances were determined at 650 nm using a plate reader (Molecular Devices). Samples and blanks were prepared in quadruplicates.

Calculations. PTPase activities, based on a potassium phosphate standard curve, were expressed as nanomoles of phosphate released/min/mg protein. Inhibition of recombinant h-PTP1B by test compounds was calculated as percent of phosphatase control. A four-parameter nonlinear logistic regression of PTPase activities using SAS release 6.08, PROC NLIN, was used for determining IC₅₀ values of the test compounds. The reported IC₅₀ values show significant fit to the regression curve (*p* < 0.05).

ob/ob Diabetic Mouse Model. Experimental details for the ob/ob diabetic mouse model were previously described.[33]

X-ray Crystallographic Studies: Protein Production, Crystallization, and Data Collection. Human recombinant PTP1B catalytic domain (residues 1−299) was prepared as described.[34] Complex solution was made by mixing excess of inhibitor dissolved in DMSO with protein (protein:inhibitor = 1:1.5 ~ 3.0), incubated at room temperature for at least 3 h, then filtered with 0.1 μm filters. Crystals of h-PTP1B−inhibitor complex were obtained by vapor diffusion at 4 °C using 0.1 M HEPES, (pH 7.5), 50 mM MgCl₂, 18% PEG 4000, 3 mM DTT, and 10~15 mg/mL protein. Typically, rodlike crystals appeared overnight and continued to grow to a maximum size of 0.4 mm × 0.2 mm × 0.7 mm within 10 days. The crystals belonged to space group *P*3(1)21, *a* = *b* = 88 Å, *c* = 104 Å, α = β = 90°, γ = 120°. The crystals were cryoprotected by transferring into the crystallization solution plus 30% glycerol. Cryoprotected crystals were flash cooled in a gaseous nitrogen stream at 100 K prior to data collection.

Diffraction data of the h-PTP1B-inhibitor complex crystals were collected by in-house conventional X-ray generator using Raxis-II image detectors. All data were collected at 100 K and processed with DENZO/SCALPACK in Data Collection and Procession.[35] *R*-merge for h-PTP1B-compound **182** is 4% (resolution 40−2.0 Å, coverage = 94.6%) and for h-PTP1B-compound **80** is 4.6% (resolution 40−1.85 Å, coverage = 92.2%).

Refinement. These structures were solved by molecular replacement with the h-PTP1B catalytic domain structure model (PDB code). The area around residues 179−185 was rebuilt based on the difference density, since there was a large conformational change upon the inhibitor binding. Cycles of model rebuilding and refinement were carried out with a X-PLOR (Version 3.1, Brunger, A. T., 1992), a system for X-ray crystallography and NMR (New Haven: Yale University Press) and QUANTA. Inhibitor was built into the difference density after the first cycle of refinement. Water molecules were assigned according to F_o-F_c maps. The final model for h-PTP1B-compound **182** contained residues 1−299 and 77 waters. It exhibited good stereochemistry, with an averaged bond length and bond angle deviation from ideal geometry of 0.017 Å and 1.868°, respectively. One hundred percent of all the residues were in the most favorable orientation and the allowed regions of a Ramachandran plot. The overall *R*-factor is 22.3%, and R-free is 26.2% with 8% test reflections using diffraction data between 20 and 2.0 Å. The final model for h-PTP1B-compound **80** contained residues from 1 to 298 and 165 water molecules. The rms deviation for bond length and angle are 0.006 Å and 1.35°, respectively. One hundred percent of all residues are in the most favorable orientation and the allowed regions of a Ramachandran plot. The overall *R*-factor is 22.2% using diffraction data between 40 and 1.85 Å.

References

(1) DeFronzo, R. A.; Bonadonna, R. C.; Ferrannini, E. Pathogenesis of NIDDM. *Diabetes Care* **1992**, *15*, 318−368.

(2) Reaven, G.; Bernstein, R.; Davis, B.; Olefsky, J. M. Nonketonic Diabetes Mellitus: Insulin Deficiency or Insulin Resistance? *Am. J. Med.* **1976**, *60*, 80.

(3) Reaven, G. Role of Insulin Resistance in Human Disease. *Diabetes* **1988**, *37*, 1595−1607.

(4) (a) Goldman, J. M. Oral Hypoglycemic Agents: An Update of Sulfonylureas. *Drugs Today* **1989**, *25*, 689−695. (b) Kolterman, O. G.; Prince, M. J.; Olefsky, J. M. Insulin Resistance in Non-Insulin Dependent Diabetes Mellitus. Impact of sulfonylureas agents in vivo and in vitro. *Am. J. Med.* **1983**, *74* (Suppl. 1A), 82−101. (c) Ferrannini, E. The Insulin resistance Syndrome. *Curr. Opin. Nephrol. Hypertens.* **1992**, *1*, 291−298.

(5) (a) Matsumoto, K.; Miyake, S.; Yano, M.; Tominaga, Y. Increase of Lipoprotein (a) with Troglitazone. Lancet **1997**, *350*, 1748−1749. Additional information in *Scrips* **1997**, *2282*, 21, and *Scrips* **1997**, *2292*, 20. (b) Troglitazone is being marketed in the United States as Rezulin and in Japan as Noscal.

(6) Haring, H. U. The Insulin Receptor: Signaling Mechanism and Contribution to the Pathogenesis of Insulin Resistance *Diabetalogia* **1991**, *34*, 848.

(7) (a) Goldstein, B. J. Protein-Tyrosine Phosphatases and the Regulation of Insulin Action. *J. Cell. Biochem.* **1992**, *31*, 33−42. (b) Goldstein, B. J. Regulation of Insulin Receptor Signaling by Protein-Tyrosine Dephosphorylation. *Receptor* **1993**, *3*, 1−15. (c) Ahmad, F.; Goldstein, B. J. Purification, Identification and Subcellular Distribution of Three Predominant Protein-Tyrosine Phosphatase Enzymes in Skeletal Muscle Tissue. *Biochim. Biophys. Acta* **1995**, *1248*, 57−69.

(8) McGuire M. C.; Fields, R. M.; Nyomba, B. L.; Raz, I.; Bogardus, C.; Tonks, N. K.; Sommercorn, J. Abnormal Regulation of Protein Tyrosine Phosphatase Activities in Skeletal Muscle of Insulin-Resistant Humans. *Diabetes* **1991**, *40*, 939.

(9) Myerovitch, J.; Baker, J. M.; Kahn, C. R. Hepatic Phosphatyrosine Phosphatase Activity and Its Alterations in Diabetic Rats. *J. Clin. Invest.* 1989, *84*, 976.

(10) Sredy, J.; Sawicki, D. R.; Flam, B. R.; Sullivan, D. Insulin Resistance Is Associated With Abnormal Dephosphorylation of a Synthetic Phosphopeptide Corresponding to the Major Autophosphorylation Sites of the Insulin Receptor. *Metabolism* **1995**, *44*, 1074.

(11) (a) Evans, J. L.; Jallal, B. Protein Tyrosine Phosphatases: Their Role in Insulin Action and Potential Drug Targets. *Exp. Opin. Invest. Drugs* 1999, *8*, 139−160. (b) Brichard, S. M.; Bailey, C. J.; Henquin, J. C. Vanadate Improves Glucose Homeostasis in Insulin-Resistant ob/ob Mice. *Fundam. Clin. Pharmacol.* **1990**, *4*, Suppl. 1, 54S. (c) Cro, G.; Serrano J. J.; Mongold, J. J.; Tep, A.; Vian, L.; Lazaro, R. Effects of Vanadyl Derivatives on Animal Models of Diabetes. *Fundam. Clin. Pharmacol.* **1990**, *4*, Suppl. 1, 20S.

(12) Byon, J. C. H.; Kusari, A. B.; Kusari, J. Protein-Tyrosine Phosphatase-1B Acts as a Negative Regulator of Insulin Signal Transduction. *Mol. Cell Biochem.* **1998**, *182*, 101−108.

(13) Elchebly, M.; Payette, P.; Michaliszyn, E.; Cromlish, W.; Collins, S.; Loy, A. L.; Normandin, D.; Cheng, A.; Himms-Hagen, J.; Chan, C. C.; Ramachandran, C.; Gresser, M. J.; Tremblay, M. L.; Kennedy, B. P. Increased Insulin Sensitivity and Obesity Resistance in Mice Lacking the Protein Tyrosine Phosphatase-1B. *Science* **1999**, *283*, 1544−1548.

(14) Durani, N.; Jain, R.; Saeed, A.; Dikshit, D. K.; Durani, S.; Kapil, R. S. Structure−Activity Relationship of Antiestrogens: A Study Using Triarylbutenone, Benzofuran, and Triarylfuran Analogues as Models for Triarylethylenes and Triarylpropenones. *J. Med. Chem.* **1989**, *32*, 1700−1707.

(15) Miyaura, N.; Suzuki, A. Palladium-Catalyzed Cross-Coupling Reactions of Organoboron Compounds. *Chem. Rev.* **1995**, *95*, 2457−2483.

(16) Cabiddu, S.; Cancellu, C.; Floris, C.; Gelli, G.; Melis, S. Meta-lation Reactions; Part XI. A Novel, One-Step Synthesis of Benzo-[*b*]thiophene derivatives. *Synthesis* **1998**, 888−890.

(17) Keck, G. E.; McHardy, S. F.; Murry, J. A. Some Unusal Reactions of Weinreb Amides. *Tetrahedron Lett.* **1993**, *34*, 6215−6218.

(18) Mutaitis, C. F.; Patragnoni, R.; Goodkin, G.; Neighbour, B.; Obaza-Nutaitis, J. Reduction of Heterocyclic Alcohols With Sodium Borohydride-Trifluoroacetic Acid. Preparetaion of bis-Heterocyclic Methanes. *Org. Prep. Proc. Int.* **1991**, *23*, 403−411.

(19) Todd, D. The Wolff−Kishner Reduction. *Org. React.* **1948**, *4*, 378.

(20) Hughes, D. L. The Mitsunobu Reaction. *Organic Reactions*; John Wiley & Sons Publishers: New York, 1992; pp 335−656.

(21) Goldenberg, C.; Binon, F.; Gillyns, E. Recherches Dans La Serie Des Benzofurannes. XVIII. Synthese De Benzofuryl-3, -4, -5, -6, -7 Aminoethanols. *Chim. Three.* **1966**, 221−227.

(22) Kursanov, D. N.; Parnes, Z. N.; Loim, N. M. Applications of ionic Hydrogenation to Organic Synthesis. *Synthesis* **1974**, 633−655.

(23) Asakura, J.; Robins, M. J. Cerium(IV)-Mediated Halogenation at C-5 of Uracil Derivatives. *J. Org. Chem.* **1990**, *55*, 4928−4933.

(24) Houpis, I. N.; Choi, W. B.; Reider, P. J.; Molina, A.; Churchill, H.; Lynch, J.; Volante, R. p. Synthesis of Functionalized Furo-[2,3-b]pyridines via the Pd-Catalyzed Coupling of Acetylenes to Iodopyridones. Preparation of a Key Intermediate to a New HIV Protease Inhibitor L-754,394. *Tetrahedron Lett.* **1994**, *25*, 9355−9358.

(25) Bhatt, M. V.; Reddy, G. S. A New Synthesis of Oxazoles. *Tetrahedron Lett.* **1980**, *21*, 2359−2360.

(26) Barford, D. P.; Keller, J. C.; Flint, A. J.; Tonks, N. K. Purification and Crystallization of the Catalytic Domain of Human Protein Tyrosine Phosphatase 1B Expressed in *Escherichia coli. J. Mol. Biol.* **1994**, *239*, 726−730.

(27) Ramachandran, C.; Aebersold, R.; Tonks, N. K.; Pot, D. A. Sequential Dephosphorylation of a Multiply Phosphorylated Insulin Receptor Peptide by Protein Tyrosine Phosphatases. *Biochemistry* **1992**, *31*, 4232−4238.

(28) Lanzetta, P. A.; Alvarez, L. J.; Reinach, P. S.; Candia, O. A. An Improved Assay for Nanomolar Amounts of Inorganic Phosphate. *Anal. Biochem.* **1979**, *100*, 95−97.

(29) Barford, D. J.; Flint, A. J.; Tonks, N. K. Crystal Structure of Human Protein Tyrosine Phosphatase 1B. *Science* **1994**, *263*, 1397−1404.

(30) SYBYL 6.5, Tripos Inc., 1699 South Hanley Rd., St. Louis, Missouri, 63144, USA.

(31) Heiden, W.; Goetze, T.; Brickmann, J. *J. Comput. Chem.* **1993**, *14*, 246.

(32) Barford, D.; Jia, Z.; Tonks, N. K. Protein Tyrosine Phosphatases Take Off. *Nature Struct. Biol.* **1995**, *2*, 1043−1053.

(33) Wrobel, J.; Li, Z.; Dietrich, A.; McCaleb, M.; Mihan, B.; Sredy, J.; Sullivan, D. Novel 5-(3-Aryl-2-propynyl)-5-(arylsulfonyl)-thiazolidine-2,4-diones as Antihyperglycemic Agents. *J. Med. Chem.* **1998**, *41*, 1084−1091.

(34) Hoppe, E.; Berne, P. F.; Stock, D.; Rasmussen, J. S.; Moller, N. P. H.; Ullrich, A.; Huber, R. Expression, Purification and Crystallization of Human Phosphotyrosine Phosphatase 1B. *Eur. J. Biochem.* **1994**, *223*, 1069−1077.

(35) Otwinowski, Z., Sawyer, L., Isaacs, N., Bailey, S. W., Eds. Daresbury, *U.K. Science and Engineering Council*, pp 56−62, 1993.